Renewable and Sustainable Energy Reviews 189 (2024) 113878

Contents lists available at ScienceDirect

Renewable and Sustainable Energy Reviews

journal homepage: www.elsevier.com/locate/rser

Feasibility and prospects of symbiotic storage of CO_2 and H_2 in shale reservoirs

Lei Hou [a], Derek Elsworth [b], Jintang Wang [c], Junping Zhou [d], Fengshou Zhang [e,*]

[a] China-UK Low Carbon College, Shanghai Jiao Tong University, Shanghai, 201306, China
[b] Energy and Mineral Engineering & Geosciences, EMS Energy Institute and G3 Center, Pennsylvania State University, University Park 16802, USA
[c] School of Petroleum Engineering, China University of Petroleum (East China), Qingdao, 266580, China
[d] State Key Laboratory of Coal Mine Disaster Dynamics and Control, Chongqing University, Chongqing, 400044, China
[e] Department of Geotechnical Engineering, College of Civil Engineering, Tongji University, Shanghai, 200092, China

A R T I C L E I N F O

Keywords:
CO_2 storage
Hydrogen storage
Shale
Fractures
Critical review
Case study

A B S T R A C T

Storing CO_2 and H_2 in underground reservoirs represents an effective approach to sequester increasing amounts of captured CO_2 for carbon neutrality and to store H_2 to promote clean energy revolutions. However, commercial/pilot-scale CO_2/H_2 storage sites are mainly restricted to conventional oil reservoirs or salt caverns – both capacity and geographic-location limited. This paper presents a systematic review of the feasibility and prospects of CO_2 and H_2 storage in fractured shale reservoirs as secure repositories. Both field pilot and laboratory studies of CO_2 injection in shales are cross-analyzed across various spatial and time scales, to provide a reliable and substantial basis to support new findings. The presence of suitable injectivity and adequate sealing capacity in shale are demonstrated. The fracture networks are shown to provide major storage space in shales, contrasting with the pore system in conventional reservoirs. This difference in storage mechanisms results in an overestimation in the storage capacity of shales when applying porous-medium-based methods. An underestimation in the mass of injection, however, is apparent from a single well for the reported cases due to unknown characteristics of underground fracture networks. The symbiotic storage of CO_2 and H_2 in shale is discussed in its feasibility and ability to improve both CO_2 storage but principally H_2 recovery – due to the presence of a gas cushion. A new equivalent-fracturing method is proposed as a supplement to recalibrate the over- and underestimated prospects of CO_2/H_2 storage in shales – a necessary component in reducing carbon emissions and accelerating the energy transition.

1. Introduction

Geological storage of CO_2 and H_2 are essential components in mitigating global warming and enabling the energy transition [1–4]. In 2021, global energy-related CO_2 emissions remained at 33.0 Gigatonne (Gt) [5]. For economic reasons, a survey by the Global CCS (Carbon Capture and Storage) Institute shows that almost 80 % of commercial CCS projects – 24 out of 31 as of 2022, are performed in oil reservoirs for EOR (Enhance Oil Recovery) [6]. CO_2 improves the mobility of crude oil by reducing oil viscosity, which stimulates the production and sequestration of CO_2 by replacing in-situ oil [7–9]. However, assuming that all the produced oil is replaced by CO_2, the global CO_2 storage (4.2 Gt in 2021, ignoring the density difference between CO_2 and oil) is still far below (~13 %) the required annual storage demand (33.0 Gt) [10]. Meanwhile, a different situation but maybe the same solution exists in the development of geological storage for H_2 [11,12]. Initially tested in salt caverns, more exploration in a broader suite of potential repository geological environments is critical for H_2 storage to improve volume capacity and stability [13–16], promote investment for construction [17–21], and bridge the disparate spatial range of storage sites and scattered market distribution [4,22,23]. Therefore, the available capacity of repositories requires an expansion of geological storage for both CO_2 and H_2, in order to meet the increasing demand for carbon neutrality and promote the clean energy transition.

Shale reservoirs can be optimized for storing CO_2 and H_2. Prospective resources in shale comprise an estimated 7576.6 trillion cubic feet of gas and 418.9 billion barrels of oil – far in excess of current worldwide reserves (293 billion barrels) as assessed by the Energy Information Administration (EIA) [24,25]. Interestingly, China and the U.S., heading

* Corresponding author.
E-mail address: fengshou.zhang@tongji.edu.cn (F. Zhang).

https://doi.org/10.1016/j.rser.2023.113878
Received 27 March 2023; Received in revised form 18 September 2023; Accepted 9 October 2023
Available online 27 October 2023

Nomenclature

Abbreviations

CO_2	Carbon dioxide
H_2	Hydrogen
CH_4	Methane
CCS	Carbon capture and storage
EOR/EGR	Enhanced oil/gas recovery

Units

Gt	Gigatonne
MPa	Megapascal
PSI	Pounds per square inch
m^3	Cubic meter
kg/m^3	Kilogram per cubic meter
m	Meter
m^3/min	Cubic meter per minute
USD/kg	US dollar per kilogram
mD	Millidarcy
gpm	Gallons per minute

the CO_2 mission country list, also lead in the development of, and production from, shale reservoirs [5,26]. Large reserves with broad geographic distribution and active investment potentially favor CO_2 and H_2 storage in shale [27–30]. Moreover, the extremely low permeability of the shale matrix in naturally fractured reservoirs enhances the intrinsic safety of CO_2 and H_2 storage by constraining migration [31–34]. Used as a working fluid, CO_2 can improve the efficiency of oil/gas recovery in shale by creating and accessing more complex fracture networks [35–38], replacing CH_4 with its higher adsorption capacity [39–42] and reducing oil viscosity for miscible displacement [43–46].

Mechanisms of fluid storage (in-situ oil/gas and injected CO_2/H_2) in shale are different from those in conventional porous reservoirs [47]. Conventional reservoirs for oil and gas usually comprise a connected pore system within highly permeable rocks (millidarcy level) that are sealed by an impermeable caprock to provide structural (anticline and fault) and/or stratigraphic (facies change) traps [48–50]. Thus, conventional reservoirs store CO_2 and H_2 in the same way as trapping oil and gas [51–53]. However, shale reservoirs contain oil and gas as a result of their nano-darcy-level permeability – maybe six orders of magnitude lower than the permeability of conventional reservoirs [54–56]. Shale reservoirs have to be artificially fractured by massive hydraulic fracturing to create conductive fracture networks before production may begin [57–59]. This artificial intervention generates a fracture-pore system for oil and gas production that is then available for the subsequent storage of CO_2 and H_2 and which is significantly more complex than the connected pore system in conventional reservoirs [60–63]. The adsorption, dissolution and diffusion behaviors of CO_2 in shale fractures and matrix represent the basic mechanisms for its permanent storage. Although a few field pilots for CO_2 storage in shale have been conducted, a significant gap still exists between lessons learned from field pilots and laboratory studies [64–68] – for instance, the limited injection scales in situ and the enormous estimated storage capacity. Currently, the idea of storing H_2 in shale is more conceptual. Research work mainly assesses sealing performance in shale and the periodic injection-recovery performance [69], which is one of the major differences compared with the permanent storage of CO_2. Therefore, technical innovations and more targeted research are needed to advance the commercialization of CO_2 and H_2 storage in shale reservoirs.

This paper provides a comprehensive review and analysis of CO_2 and H_2 storage in shale. First, field-scale pilots of CO_2 injection in shales are summarized. Their feasibility is demonstrated by confirming the injectivity of CO_2 in fractured and intact shales and by noting the sealing performance of the shale matrix. Second, a critical review of relevant literature, focusing on the outcomes and lessons-learned from field pilots, is summarized to delineate principle mechanisms of CO_2/H_2 injection and storage. Then, analyses synthesizing field tests and laboratory studies are conducted and reported to generate critical perspectives. Recommendations for CO_2 and H_2 storage in shale reservoirs are proposed to improve both the estimation of storage capacity and the efficiency of field pilots – a credible technology pathway to carbon neutrality and new energy transition.

2. Field pilots – feasibility and observations

Field demonstration projects play a crucial role in the development of rational methods for subsurface storage by surmounting the intrinsic scale limitation of laboratory research [70–72]. Typical cases of CO_2 injection in unconventional shale formations are summarized and analyzed to validate the feasibility of the approach and summarize important observations. As an adjunct, geological storage of H_2 in shale is currently conceptual [73–75], but may be advanced through documenting experiences of CO_2 injection because of the similarity of the anticipated injection process and anticipated reservoir conditions.

2.1. Field records of CO_2 and H_2 storage

Injecting CO_2 into oil and gas reservoirs to improve production can be traced back to the 1980s inclusive of the use of CO_2 foams, energized fracturing fluids and other approaches [76–78]. Representative cases are summarized in chronological order in Table 1 by restricting the consideration to shale reservoirs and pure-CO_2 injection. Cases 1–4 are early attempts in Bakken and Chattanooga shales in North America since 2008 [79]. Cases 5–7 are recent pilot studies in China using CO_2 as hybrid fracturing fluids (Table 1). All cases are operated by energy companies with the desire to develop a generic and improved stimulation technique. CO_2 is injected into both artificially-fractured and initial-intact shale reservoirs for enhanced oil/gas recovery (EOR/EGR) and permanent sequestration of CO_2. The phase of the CO_2 is initially liquid and is transformed into either gaseous or supercritical states depending on the pressure and temperature of reservoirs [80–84]. The scale of these injections varies between ~100 and 3000 tons for a single well. The injection rate is typically measured in days for huff and puff injections (Cases 1–3, Table 1) and in minutes for hydraulic fracturing injections (Cases 5–7, Table 1). Correspondingly, the wellhead pressure is much lower in the huff and puff cases (~3.45 MPa) than for hydraulic fracturing (~60 MPa). This paper focuses on storing CO_2 in shale when analyzing field tests and fundamental research, for instance, in examining injectivity, sealing performance and migration, among other parameters. The aspects of enhanced oil and gas recovery by CO_2 are not the focus of this study.

The concept of H_2 storage is discussed together with that of CO_2 storage since the case for H_2 storage in shale is rarely reported. The geological storage of H_2 is mainly restricted within salt caverns, as shown in Table 2. Noteworthy, is that CO_2 is a common impurity during hydrogen production, for instance, grey hydrogen (H_2) obtained from the gasification of coal. Low-purity H_2, mixed with CH_4, N_2, CO and CO_2, is used as town gas in European projects (Germany, France and Czech Republic), as presented in Table 2. Although CO_2 is not injected by design in H_2 storage sites, the geological coexistence of CO_2 and H_2 is feasible based on field pilots. Further laboratory studies show that the injection of CO_2 as a cushion gas can boost reservoir pressure, prevent water breakthrough, and then enhance the recovery and purity of H_2 production in salt caverns and aquifers [53,73,75]. Moreover, our previous studies indicate that the adsorption of CO_2 onto organics and clays swells the shale matrix and potentially reduces fracture permeability – sometimes significantly [40,85,86]. Therefore, high contents of organics and clays in shales (a unique feature compared with salt caverns or

Table 1
Summary of CO_2 injection cases in shale reservoirs [64–68].

No.	Case 1	Case 2	Case 3	Case 4	Case 5	Case 6	Case 7
Year	2008	2009	2014	2017	2017	2018	2019
Well No.	NDIC 16713	Burning Tree-State 36-2H	Hw-1003	Knutson-Werre 34-3WIW	Yan-2011	BYY-1HF	Jiye-1HF
Operator	EOG Resources, Inc.	Continental Resources/XTO Energy	VCCER/Cardno Ltd/ FloCO2	EERC/XTO Energy	Yanchang Oil	SINOPEC	PetroChina
Location	Parshall Field, North Dakota	Elm Coulee Field, Montana	Boone Camp Field, Tennessee	Dunn County, North Dakota	Ordos Basin, Shaanxi	Jianghan Oilfield, Hubei	Jilin Oilfield, Jilin
Formation	Upper Bakken Shale	Middle Bakken Shale	Chattanooga Shale	Middle Bakken Shale	Yanchang Formation Shale	Qianjiang Formation Inter-salt Shale	Qingshankou Formation Shale
Depth	–	–	~1120 m	~3337 m (MD[a])	~2940 m	~3358 m	2420–2500 m
In-situ Fluid	Oil	Oil	Gas	Oil	Gas	Oil	Oil
Reservoir Integrity	Fractured	Fractured	Fractured	Intact	Intact	Intact	Intact
Well Completion	Horizontal/6 stages	Horizontal/ single stage	Horizontal/4 stages	Vertical well	Vertical well	Horizontal/5 stages	Horizontal/18 stages
CO_2 Injection Scale	1325 tons	2570 tons	510 tons	99 tons	386 m^3	1564 m^3	3265m^3
Stimulation Type	Huff and puff	Huff and puff	Huff and puff	Injectivity test	Fracturing	Fracturing	Fracturing
Fluid Component	Pure CO_2	Pure CO_2	Pure CO_2	Pure CO_2	Pure CO_2 & gel	Pure CO_2 & gel	Pure CO_2 & gel
Injecting Rate	–	132.5 tons/day	40.95 tons/day	25 tons/day	~2 m^3/min[b]	~4.8 m^3/min[b]	~4 m^3/min[b]
Wellhead Pressure	–	–	~3.45 MPa	~28.8 MPa[c]	~20 MPa	~60 MPa	~52 MPa
Soaking Period	–	30 days	120 days	15 days	–	26 days	–
EOR/EGR	–	Increased by ~110 %	Increased by ~15 %	–	Increased by ~50 %	Increased by ~120 %	16.4 m^3/d
CO_2 Recovery	–	50 % in 3 months	41 % in 17 months	–	~2 % of CO_2 in total produced gas	–	–
Sealing behavior/CO_2 Breakthrough	One far offset well is affected, but three nearby wells are not.	No offset-producing wells are affected.	No tracer (SF6 and PFTs) is detected from any offset wells.	The injectivity of the Bakken shale is relatively low.	–	Micro-seismic events are observed during CO_2 injection.	Micro-seismic events are observed during CO_2 injection.
Other Observations [d]	Local natural fracture system may dominate the breakthrough.	–	CO_2 exists as gaseous in the reservoir.	Production of light-oil increases. No fracture is generated.	–	Production of light-oil increases.	Less volume of CO_2 is needed to generate a micro-seismic event.

* The units of field measurements are unified for comparison.
[a] **MD** – measured depth, is the length of the wellbore, and is greater than the vertical depth.
[b] The unit represents the injected volume of liquid CO_2 per minute.
[c] This pressure is converted from the bottom hole pressure (9500 psi) based on the MD (3337 m) and the density of liquid CO_2 (1100 kg/m^3), thus lower than the actual wellhead pressure.
[d] More details of the observations are explained in Sections 2.2 and 2.3.

Table 2
Sites for geological storage of hydrogen. Adapted with permission from Ref. [52], copyright (2021) Elsevier.

Field/Project Name	Reservoir	H_2/ %	Impurities	Working Pressure/ MPa	Depth/ m	Volume/ m^3	Status
Teesside (UK)	Bedded salt	95	~4% CO_2	4.5	365	210,000	Operating
Clements (US)	Salt cavern	95	–	7.0–13.7	1000	580,000	Operating
Moss Bluff (US)	Salt cavern	–	–	5.5–15.2	1200	566,000	Operating
Spindletop (US)	Salt cavern	95	–	6.8–20.2	1340	906,000	Operating
Kiel (Germany)	Salt cavern	60	~30 % of N_2, 10–33 % of CH_4 and 12–20 % of CO and CO_2	8.0–10.0	–	32,000	Closed
Ketzin (Germany)	Aquifer	62		–	200–250	–	Operating
Beynes (France)	Aquifer	50		–	430	3.3×10^8	Operating
Lobodice (Czech Republic)	Aquifer	50		9.0	430	–	Operating
Diadema (Argentina)	Depleted Gas	10	–	1.0	600	–	–
Underground Sun Storage (Austria)	Depleted Gas	10	CH_4, CO_2	7.8	1000	–	Operating

aquifers) may enhance the cushion-gas function of CO_2 to restrain H_2 leakage and boost the recovery rate – this observation inspires a potential strategy for the symbiotic storage of CO_2 and H_2 in shales.

2.2. Injectivity of CO_2 in fractured and intact shales

The feasibility of injectivity of CO_2 is a prior concern for shale reservoirs because of their initial nano-scale permeability [87,88], which elevates injection pressures and then influences the efficiency (operation period) and economics (usage of pumps and wellhead) of CO_2 storage. For artificially fractured reservoirs, 128–2570 tons of CO_2 can be injected for one stage of a horizontal well (Cases 1–3). This number is approximately 199~344 tons/stage for an unfractured shale reservoir (Cases 6 and 7) [66,68]. Even at the smallest scale (510 tons in total), the amount of injected CO_2 for Case 3 is close to the historical hydraulic fracturing scale (amount of previously injected fluid) [64]. The hydraulic injection history for Case 3 is presented in Fig. 1. The average injection rate is ~40 tons/day, which is lower than typical fracturing operations (Cases 5–7) but higher than injection tests in unfractured shale (Case 4) [65]. The wellhead pressure increases slowly and remains lower than 500 psi (3.45 MPa). CO_2 may be injected into existing fractures considering the high pressure for CO_2 to penetrate or fracture the intact shale matrix in Cases 4–7.

Injection of CO_2 in an intact shale reservoir requires greater hydraulic power, resulting in higher wellhead pressures, as shown in Fig. 1. In Case 4, downhole gauges are applied to measure the reservoir pressure and temperature during the test. The pressure in Case 4 represents the bottom-hole pressure and is slightly higher than the pore pressure (8668 psi), which is insufficient to induce fracture. The pressure differential, however, drives CO_2 to slowly penetrate the shale matrix in the days following injection – as evident in the diminishing wellbore pressure with time post-injection (after 15 h) in Fig. 1. The injection rate jumps between 6 and 12 gpm (0.0225–0.045 m^3/min), which is much lower than the pump rates applied in fracturing operations (Cases 5–7). However, the wellhead pressure (converted from downhole pressure based on well depth and density of liquid CO_2) approaches 28.8 MPa, indicating the difficulty in CO_2 injection into the intact shale matrix. Therefore, artificial fracture networks significantly improve the injectivity of CO_2, as evident in comparing injection pressures between Cases 3 and 4 (as shown in Fig. 1).

2.3. Sealing performance of shale

The sealing efficiency of fractured shale is another essential issue in the geological storage of CO_2 [89–91]. Pressure and production monitoring are performed in neighboring wells adjacent to the injecting well in Cases 1–3. Only one offset well one mile away from the injection well in Case 1 detects the CO_2 breakthrough during the injection, which may result from transmission through existing fractures [79]. However, three nearby wells within one-mile separation from the injection are not affected in Case 1. Suggesting that the characteristics of the local natural fracture system control this response. Neither abnormal pressure (pressure variations induced by CO_2 breakthrough) nor variation in production is reported in neighboring wells near injection in Cases 2 and 3. Hexafluoride (SF6) and two perfluorocarbon tracers (PFTs) are injected with the CO_2 in Case 3, but no tracers are detected in offset wells during the injection and soaking period (4 months), indicating the sealing performance of depleted shale reservoirs [92,93].

2.4. Fracturing efficiency and recovery of injected CO_2

Injecting pure CO_2 can generate fractures in shale by elevating the hydraulic injection power [86,94–96]. Micro-seismic interpretation in Cases 6 and 7 suggests massive rock failure events during the pre-injection of CO_2, as shown in Fig. 2 [66]. This case uses a hybrid fracturing method, where pure CO_2 and water-based fluid are injected successively (Fig. 2 a) [97]. The declining pressure under a constant injection rate before 60 min (highlighted by the yellow rectangle) in Fig. 2 (a) also indicates the creation and propagation of fractures [98, 99]. The statistics show that injection of every 6.5 m^3 of CO_2 and 30 m^3 of gel generates a single micro-seismic event, which is ~5 times more efficient in comparing CO_2 against water-based fluids [66]. The higher fracturing efficiency of CO_2 (lower volume of injected fluid to generate a microseismic event) may be due to its lower viscosity and higher diffusivity in its natural supercritical state under reservoir conditions [100–102]. Noteworthy is that the fracture length created by CO_2 fracturing is comparable with the length fractured by the following hydraulic injection, as presented in the plan views in Fig. 2 (b).

Quantifying the mass recovery of injected CO_2 is critical in terms of CO_2 storage in oil and gas reservoirs because CO_2-EOR does not necessarily favor the permanent storage of CO_2 [103–106]. CO_2 will preferentially dissolve and mix in the native reservoir-oil, and then increase production of light oil (as presented in Cases 4 and 6) – one of the core mechanisms of the CO_2-EOR technique [107–109]. Approximately 50 % of the injected CO_2 (1285 tons) is reproduced along with the oil in three months, as presented in Case 2 (Table 1). The recovery of CO_2 from shale gas formations is moderate – 41 % of the injected CO_2 in 17 months, as shown in Fig. 3 (a). The interaction between CO_2 and the shale matrix

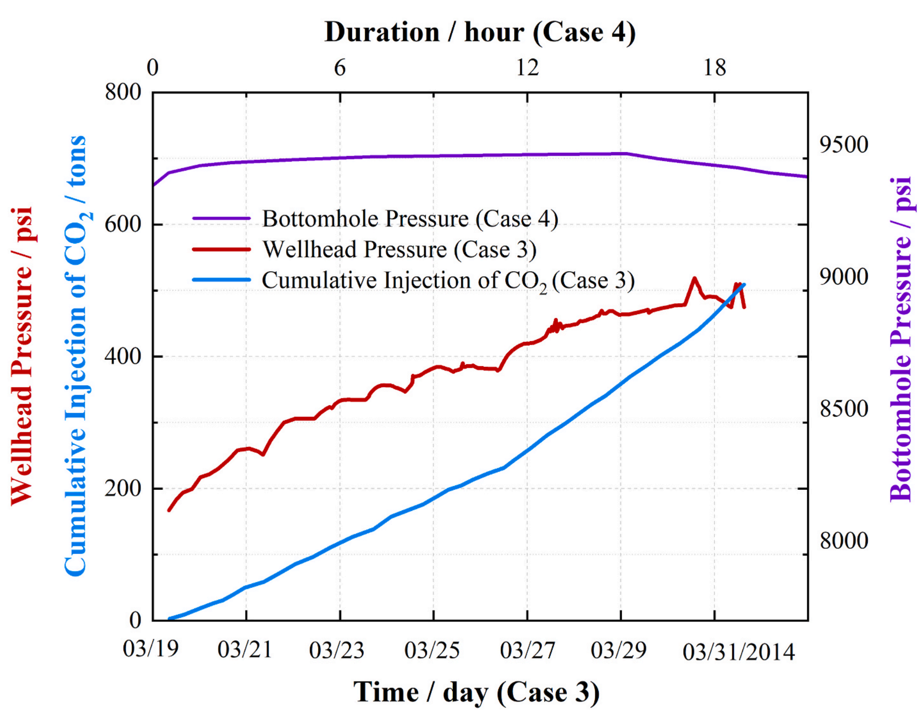

Fig. 1. The hydraulic measurements of CO_2 injection for (a) Case 3 (fractured shale reservoir) [64] and (b) Case 4 (intact shale reservoir) [65]. Redrawn with permission from Ref. [64], copyright (2017) Elsevier. (This figure has been completely redesigned and redrawn by the authors of the present manuscript).

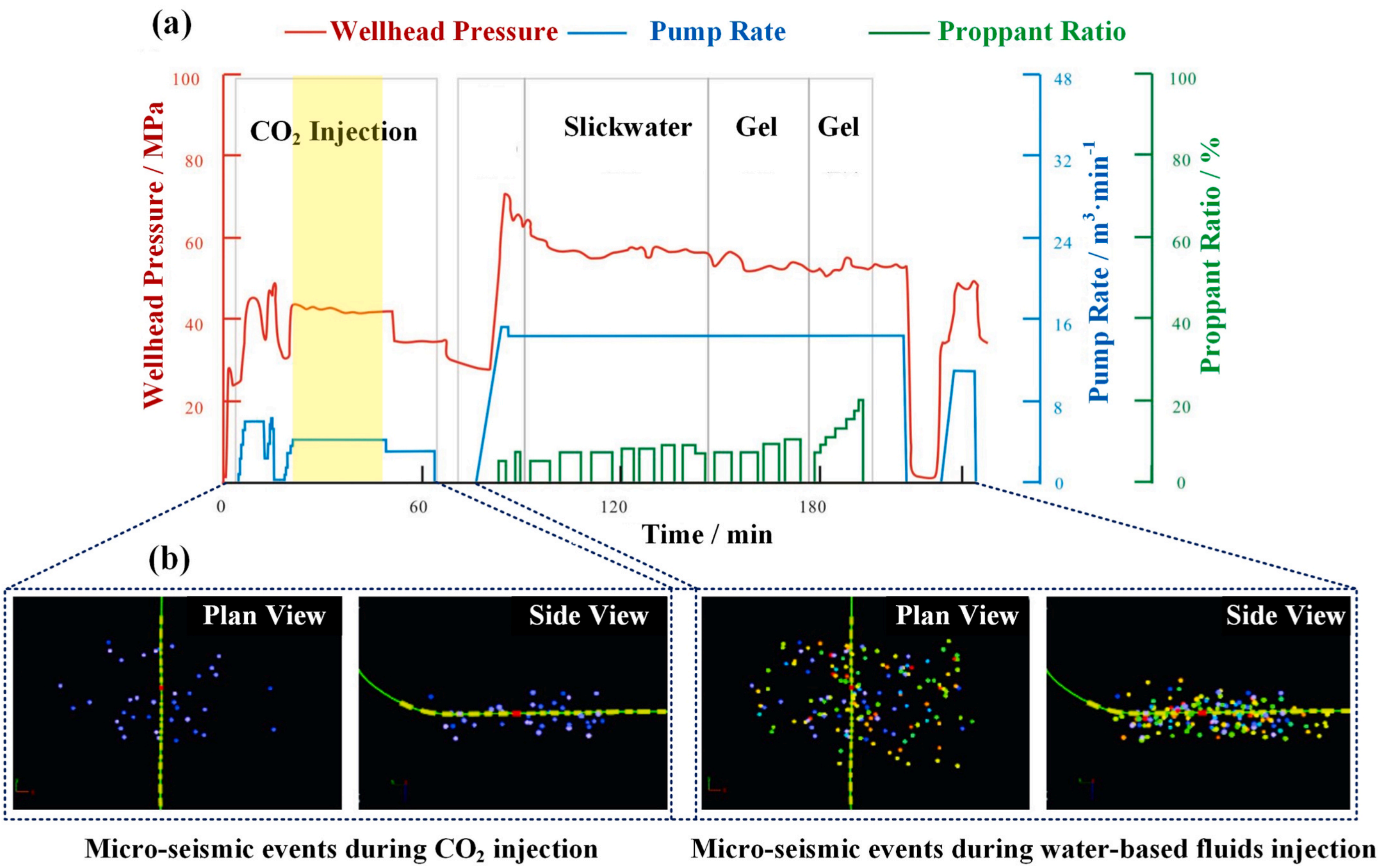

Fig. 2. Field measurements for Case 7. (a) Injection records of the 10th Stage; (b) Micro-seismic interpretations for the 14th Stage [66].

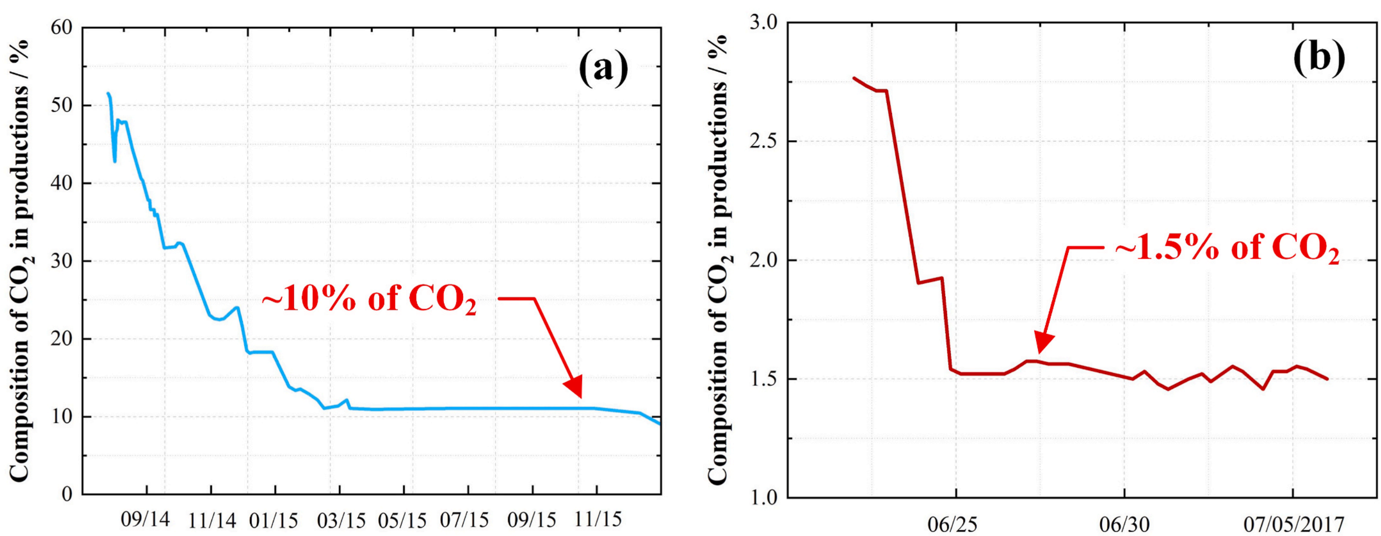

Fig. 3. Recovery of CO_2 after injections in (a) Case 3 (CO_2 huff-and-puff) [64] and (b) Case 5 (CO_2 fracturing) [67]. Redrawn with permission from Ref. [64], copyright (2017) Elsevier. (This figure has been completely redesigned and redrawn by the authors of the present manuscript).

may trap, then obstruct the flowback of CO_2, for instance, the adsorption of CO_2 onto organics and clays and their swelling effects, the dissolution of CO_2 and diagenetic reactions, among other processes [110–115]. Therefore, dry gas shale formations may be preferable for CO_2 storage compared to oil shales. Moreover, injecting CO_2 as a fracturing fluid may boost the CO_2 trap in shale. The higher injecting pressures drive CO_2 more deeply into the shale matrix from the bounding fractures. Proppant-inaccessible fractures (microfractures that allow access only for CO_2) close after fracturing injection, which will seal CO_2 in disconnected fractures. These mechanisms act against CO_2 recovery in the cases of CO_2 fracturing (~2% of CO_2 in Case 5), compared with the CO_2 concentrations for huff-and-puff injection (~10% of CO_2 in Case 3) as shown in Fig. 3.

3. Laboratory studies regarding field observations

Fundamental studies related to field tests are surveyed to define field-scale mechanisms of flow and storage, define a necessary research focus and reveal gaps between research and application. A systematic analysis is performed from the perspective of CO_2 and H_2 storage in shale, relating to storage capacity, recovery of the injected CO_2, and the feasibility of H_2 storage.

3.1. Estimation of CO_2 storage in shale

Methods of evaluation of the storage potential in conventional reservoirs are usually employed for unconventional reservoirs, which report the enormous potential of CO_2 storage in shales [34,116]. The CO_2 storage capacity in shale can be assessed either on a volumetric basis [31,117] or on a production-based basis [118]. The representative volumetric method is proposed by the United States Department of Energy National Energy Technology Laboratory (U.S. DOE NETL) [119]. The volumetric equation considers the effective reservoir area, thickness, pore volume, CO_2-sorbed volume, and gas-rock contact area. This method provides a theoretical storage capacity of CO_2 assuming 100 % of the in-situ fluids are replaced by injected CO_2 [120,121]. The production-based method is based on the same constraints of CH_4 flow out-from and CO_2 transport back-into the same formation. Models for CH_4/CO_2 sorption equilibria and kinetics are utilized together with published CH_4 production data for evaluation [118]. The volumetric approach has been previously used to estimate the CO_2 storage capacity in the Ohio and New Albany shales (~28 Gt) [122], and in the Marcellus shale (~171 Gt) [31]. Using the production-based approach, a time-dependent curve of CO_2 storage suggests that ~18.4 Gt of CO_2 can be stored in Marcellus Shale by 2030, as shown in Fig. 4 [118].

Moreover, numeral models of shale reservoirs simulate the process of CO_2 injection and evaluate the efficiency of CO_2 storage. Different injecting models (CO_2 flooding and huff-and-puff) are tested based on mechanisms of adsorption, dissolution, diffusion, and compaction. CO_2 flooding and huff-and-puff improve gas production by 24% and 6%, respectively, based on data from the Barnett shale, which agrees with field observations (~15%) in Case 3 (Table 1). The injected CO_2 is stored in free, adsorbed and dissolved states in the proportions of 42 %, 55 %, and 3 %, respectively [123]. Moreover, CO_2 storage capacity is found to have a time dependency over the lifetime of a CO_2 storage project [124]. Research suggests that CO_2 is mainly trapped in a free state over the short term (i.e. decades), then is mineralized significantly over the long term (thousands of years) in Yanchang shale, as shown in Fig. 5 [125]. Estimation of CO_2 storage in Devonian shale shows that porosity and adsorption, respectively, contribute 50 % of the storage capacity [126].

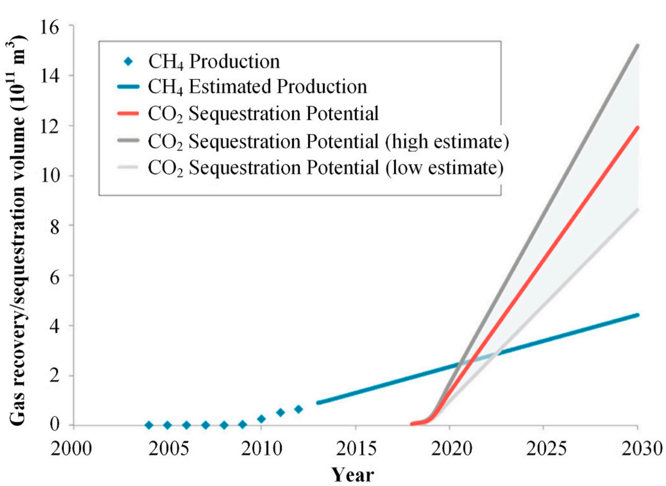

Fig. 4. Estimate of CO_2 storage capacity in the Marcellus shale based on historical and projected CH_4 production. The high and low estimates represent 1 standard deviation. Reprinted with permission from Ref. [118], copyright (2013) American Chemical Society.

3.2. Efficiency of CO_2 storage – recovery issue

The co-recovery of CO_2 together with oil and gas is a severe issue in a producing reservoir (Cases 2 and 3, Table 1), which may determine the efficiency of permanent CO_2 sequestration. However, injecting CO_2 to enhance oil and gas recovery (EOR/EGR) is currently the most economic and frequent way to perform CO_2 storage in reservoirs [127–130]. Numerical simulations, combing micro-seismically-interpreted fracture networks, predict a CO_2 storage efficiency (ratio of sequestrated and injected CO_2) as low as 21.3 % after 20 years for one cycle of huff-and-puff injection in Longmaxi shale, in China [131]. The efficiency of CO_2 storage may be improved by performing continuous injection-production cycles, annually. Starting from ~20 %, the efficiency increases continuously and approaches ~90 % by 30 years in both Bakken oil shale (Fig. 6 a) and the Eagle Ford gas shale (Fig. 6 b) [132]. The average efficiency of CO_2 storage varies between 30 % and 80 % depending on the specific reservoir and injection schedule. The selection of injection pressure is observed to dominate the efficiency among the engineering and geological factors (injection rate, injection time, number of cycles, carbon dioxide soaking time, fracture half-length, fracture conductivity, fracture spacing, porosity, permeability, and initial reservoir pressure), as shown in Fig. 6.

3.3. Feasibility of H_2 storage in shale

Candidates for the geological storage of H_2 (including salt and rock caverns, saline aquifers, and depleted oil and gas reservoirs) are analyzed from the perspectives of capacity, stability, cost and transport to highlight the feasibility of H_2 storage in shales [133–135]. As a valuable fuel, pilot tests of H_2 storage are mainly performed in salt caverns to control the dissipation and purity (Table 2). However, unique advantages and perspectives of H_2 storage in shale are apparent in the aspects of capacity, stability, cost and transport. For inter-seasonal storage and adjustment, porous depleted reservoirs can offer capacities several orders of magnitude larger than salt caverns [52,69,74]. This storage capacity is also more stable in rock-based reservoirs than the capacity in salt caverns that are subject to deformation and fatigue damage and failure of salt under cyclic loading [136–138]. The costs of geological H_2 storage in different underground storage sites may be analyzed and compared. The most economical candidate is depleted reservoirs at 1.23 USD/kg of stored H_2, followed by aquifers at 1.29 USD/kg, then caverns at 1.61–2.77 USD/kg for salt and hard rock caverns [139]. Among depleted reservoirs, the construction and operation costs are lower for depleted gas reservoirs than the costs for depleted oil reservoirs [23]. Moreover, oil and gas reservoirs are more widely and ubiquitously distributed than the limited geological location-specific salt cavern sites that are potentially far from markets. Recycling pre-existing oil and gas infrastructure for H_2 production and transport can furthermore save on the necessarily large capital investment. A comprehensive benchmarking result of different underground options is presented in Fig. 7, suggesting that salt caverns, depleted gas reservoirs and aquifers (ranking from the first to the third) are preferential considering safety, feasibility, cost and operation [140].

H_2 storage in gas shale reservoirs is investigated *via* reservoir simulations (as shown in Fig. 7) to reveal the contributions of matrix permeability, injection scale, and period length of the injection cycle on the recovery and purity of H_2. The simulation results, focusing on Haynesville shale, indicate that H_2 recovery increases from 35.2% for a short-term (12 h) cycle to 68.7 % for an intermediate-term (30 days) cycle, both for large-scale (thousands of tons of H_2) injections [69]. For small-scale (hundreds of tons of H_2) injections, the recovery efficiency increases from 44.7 % for a short-term cycle to 71 % for a long-term (120

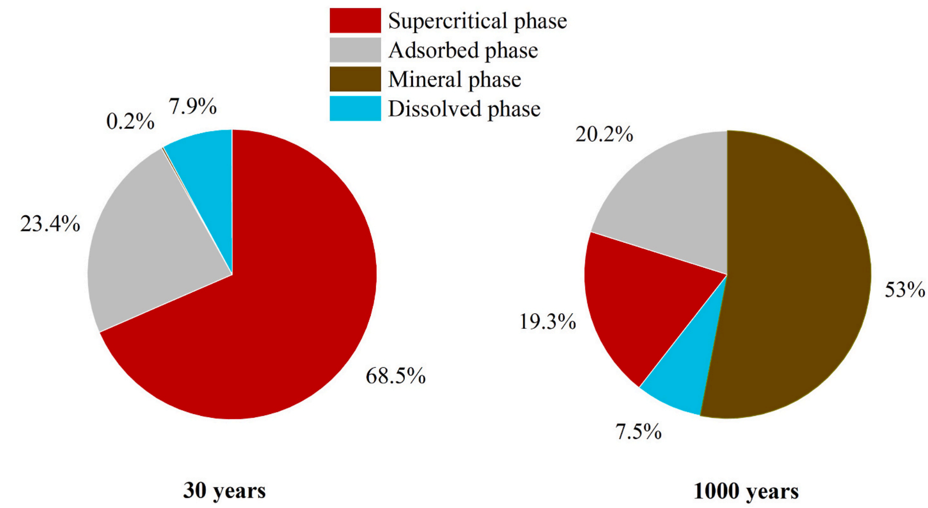

Fig. 5. Proportions of stored CO_2 in different phases in Yanchang shale after 30 years and 1000 years. Redrawn with permission from Ref. [125], copyright (2016) Elsevier.

days) cycle, which is mainly dominated by the well shut-in and pressure build-up due to the remaining methane [69]. Without aid from a gas cushion (for instance, CO_2, CH_4, or other gases), this recovery is comparable to the estimated recovery of H_2 from conventional reservoirs (50 %~87 %) [74] and saline aquifers (~78 %) [141]. The tightness of the shale matrix remains essentially impermeable to H_2 (H_2 penetrates only marginally into the matrix) when the matrix permeability is lower than 0.001mD [69]. Hydrogen is, therefore, mainly stored within hydraulic fractures. Moreover, shale gas reservoirs are usually dry when devoid of water production, which mitigates the H_2-hysteresis mechanisms, such as relative permeability [142], capillary pressure [93], interfacial tension [143–145], and contact angles [146].

4. Cross-validation and critical reviews

Observations of field tests and laboratory studies are summarized and cross-analyzed for critical perspectives and definitions of new mechanisms and methods, as shown in Fig. 8. Field pilots have demonstrated the feasibility (injectivity and sealing performance) of CO_2 storage in shales. Laboratory studies reveal the mechanisms and extrapolate the time scales of CO_2 injection. This comprehensive analysis of field and laboratory evaluations provides an integrated review of mechanisms and outcomes.

4.1. Overestimation of CO_2 storage capacity in shale

Porous-medium-based methods applied to conventional reservoirs are often inappropriately employed in assessing the storage capacity in unconventional shales (fracture-dominant) – potentially resulting in overestimation, as illustrated in Fig. 9. Both volumetric and production-based methods evaluate CO_2 storage capacity based on the "dual porosity – with fractures for flow and matrix for storage" feature of shales [117,119,122]. The fractures (natural and artificial fracture networks) in shale provide a high-conductivity flow path for the initial high rate of production of oil or gas [57,147]. However, production rates soon drop dramatically as fractures are drained, followed by a slow fall-off of production as oil/gas migrates from the matrix to fractures [148–150]. Current evaluation methods assume that the injected CO_2 would follow the reverse path – quickly filling the fracture networks and then penetrating into the matrix [118,119]. This assumption is tenable for conventional reservoirs with high permeability (millidarcy level) and connected-macro/micropore systems in the rock matrix (Fig. 9 a), but may fail for extremely-tight shales with nano-darcy-level permeabilities and more isolated pores in the matrix (Fig. 9 b) [151,152]. The volumetric method presumes that all in-situ fluids in the pores are replaced by CO_2, which may ignore the prerequisite of having a connected fracture network – providing a flow path [153]. Although the volumetric reach of horizontal wells and hydraulic fracturing create penetrative fracture networks, the volume of this fracture-accessible space is still small in comparison with the basin-scale reservoir volumes representing the storage capacity [58] – even taking all wells and their stimulated volumes into account. This gap results in an overestimation of CO_2 storage capacity in shale when using the volumetric evaluation method. Moreover, the recovery issue decreases the storage efficiency, which is also crucial in this overestimation.

Even with sufficiently penetrative and connected fracture networks, the penetration of CO_2 into the shale matrix will consume a significant amount of energy and evolve over an extended time, as tested in Case 4 (Fig. 1). The matrix-fracture-well flow path for oil and gas may be reversed in conventional reservoirs, which is the principal mechanism for flooding – injecting CO_2 from one well and producing oil/gas from an offset well through the matrix [154,155]. This flooding technique, however, is rarely applied to shale reservoirs because of their impermeable matrix that obstructs production in offset wells, as the monitoring observations in Cases 1–3 (Table 1). Studies also show that if a conventional reservoir can accept one standard cubic meter of CO_2 per second per square meter of the exposed wellbore, then the shale reservoir would require a million seconds (11.6 days) to accept the same amount of CO_2 under those same conditions – that is 1 s versus one million seconds [119]. Therefore, the penetration of CO_2 into a shale matrix relies on the driving energy (pressure) and time, which is also demonstrated by the high wellhead pressures apparent in Cases 4–7 (Table 1) and in the dominant influence of injection pressure in the efficiency of CO_2 storage (Fig. 6). This mechanism is neglected when deriving the production-based evaluation method, thus resulting in the overestimation [118]. The production of hydrocarbons is driven by sustaining continuous geological stress and in-situ pore pressure, while the artificial injection of CO_2 is limited by the capacities of wellhead equipment and pumps, the economic efficiency and injecting time. Consequently, storing CO_2 in fracture networks in shales may be more feasible and efficient than in the matrix, which is also observed in the numerical simulation of H_2 storage in shale [69].

4.2. Underestimation of CO_2 injection in single well

The scale of injected CO_2 in fractured reservoirs varies between 128 tons/stage and 2570 tons/stage as presented in Table 1 (Cases 1–3). Case 3, at the smallest injection scale, is designed based on the fracturing

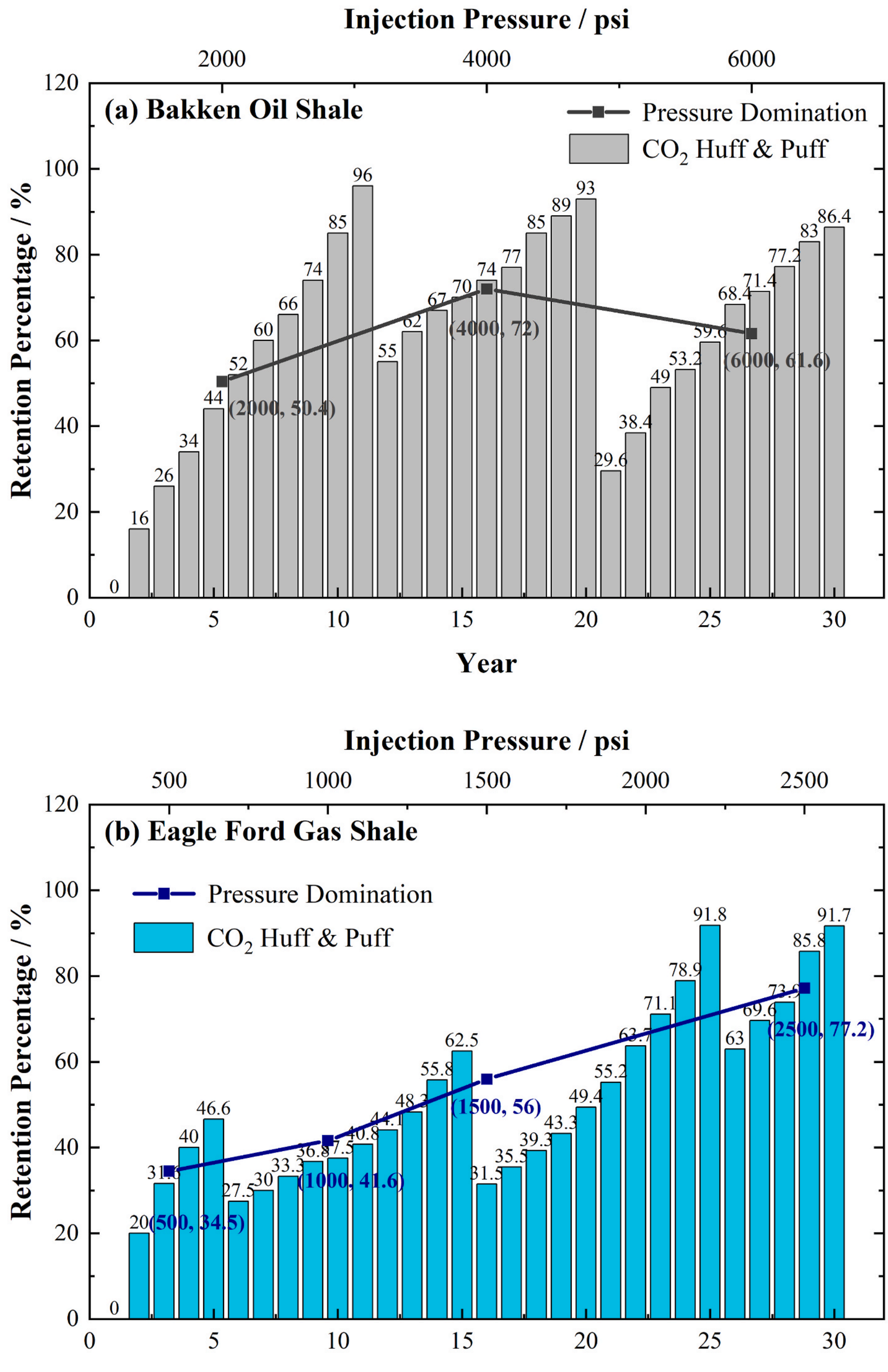

Fig. 6. Retention percentage (ratio of CO_2 remaining in the subsurface to the total injected CO_2) with respect to "Year" and "Injection Pressure" for CO_2 Huff-and-Puff injection in (a) the Bakken oil shale and (b) the Eagle Ford gas shale. Redrawn with permission from Ref. [132], copyright (2018) Elsevier.

scale, namely, the volume of injected CO_2 is approximately equal to the volume of injected fluids for the prior fracturing [64]. According to this principle, a typical stage for shale gas fracturing in the Sichuan Basin (China) consumes ~2000 m^3 of liquid [156,157], which may be equivalent to a CO_2 storage capacity exceeding 2000 tons/stage. Similarly, the scales of CO_2 injection in Cases 6 and 7 may achieve only ~19.7 % (1564 m^3 of CO_2; 7944 m^3 of total fluids) and ~9.4 % (3265 m^3 of CO_2; 34,808 m^3 of total fluids) of the capacity, respectively, and thus are underestimated. This can be further demonstrated by the low and high injecting pressures in Cases 3 and 4, respectively. The injection of CO_2 may mainly fill the fracture networks and replenish the formation pressure. If the injection scale had exceeded the maximum capacity of the fractures, CO_2 would either reactivate fractures or penetrate into the shale matrix by respectively overcoming the minimum horizontal stress and the in-situ pore pressure [158,159]. Correspondingly, the wellhead pressure should be > 3.45 MPa referring to the pressure in Case 4 (~28.8 MPa, Table 1).

This underestimation may result from the unknown characteristics of the fracture networks, the physical characteristics of CO_2 as a supercritical fluid and uncertainties in the pressures and fluids in the shale.

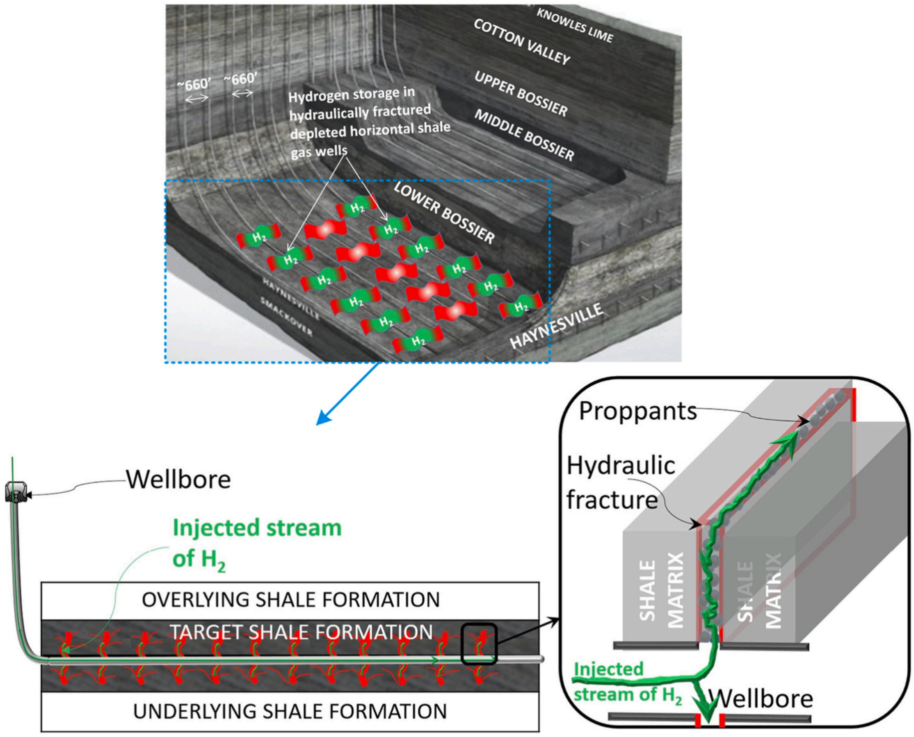

Fig. 7. Schematics of H_2 storage within hydraulic fractures, constrained by the impermeable shale matrix. The flow path of injected H_2 in a fractured depleted shale reservoir includes the wellbore and hydraulic fractures propped by proppants. Reproduced with permission from Ref. [69], copyright (2022) Elsevier.

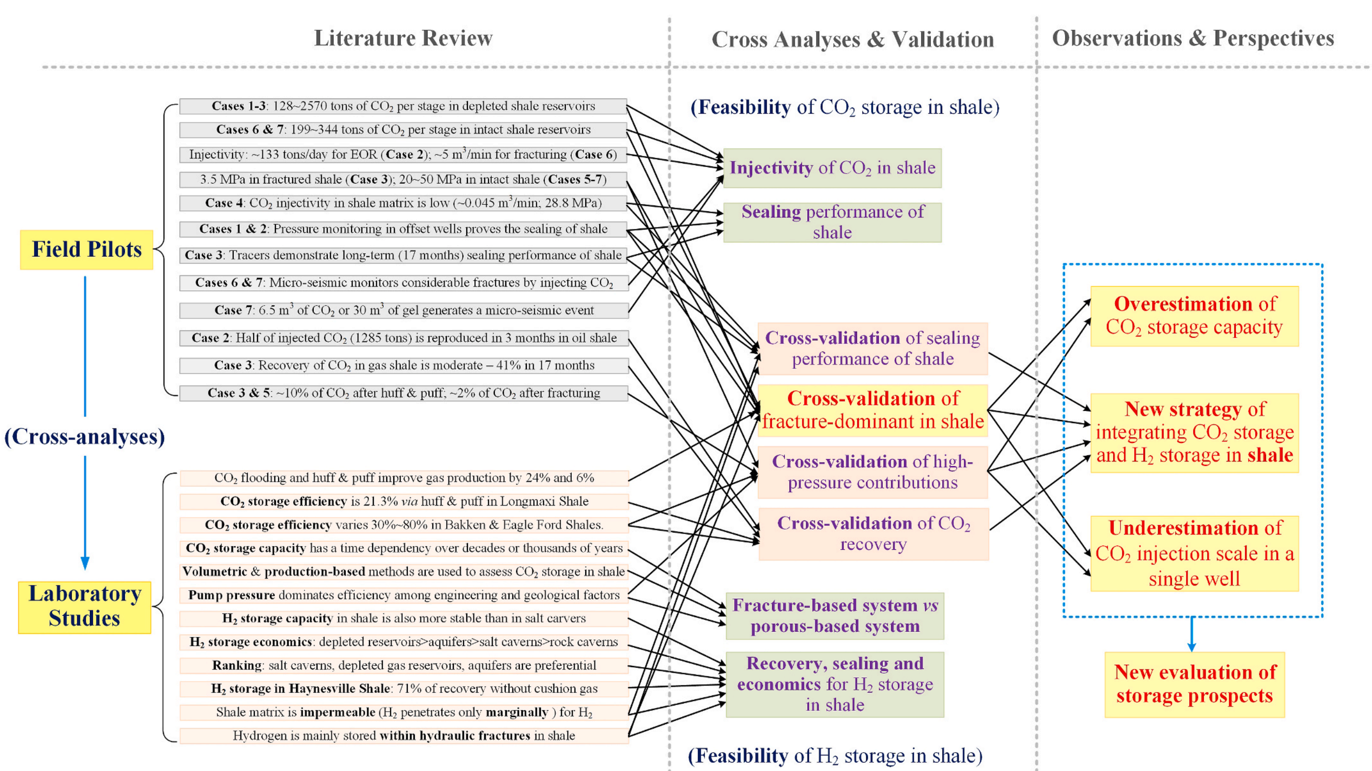

Fig. 8. Structured chart illustrating interdisciplinary analyses and cross-validation combining field pilots and laboratory studies.

The precise detection of underground fractures (several millimeters wide) in reservoirs is technically infeasible when thousands of meters away from the surface [160]. Expensive micro-seismic monitoring can only estimate the stimulated reservoir volume [161]. Thus, the complexity of fracture networks in shale exacerbates the difficulties in its characterization. Meanwhile, the high diffusivity and fully miscible and absence of a capillary exclusion pressure apparent for supercritical CO_2 enable it to access smaller fractures than does water, more

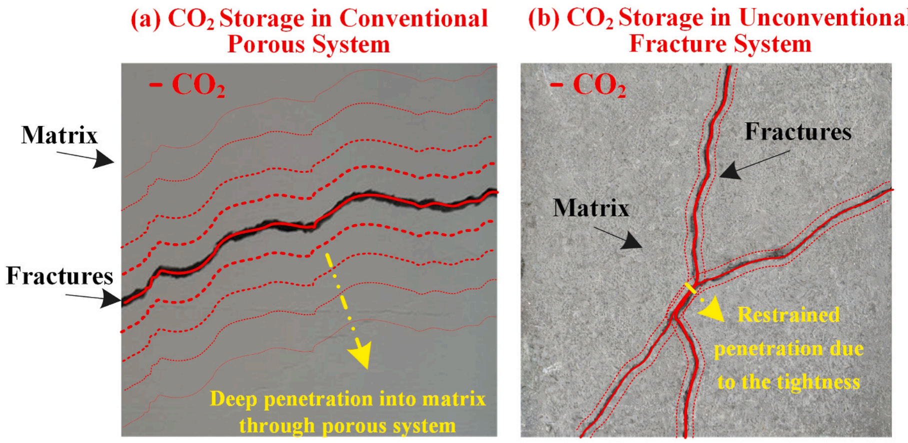

Fig. 9. Schematic of different CO_2 storage configurations and mechanisms in (a) conventional (both fractures and matrix) and (b) unconventional (mainly fractures) reservoirs. The matrix in unconventional shale reservoirs restrains the penetration of CO_2, leaving the fracture system to dominate the storage capacity – different from the conventional porous system storing CO_2 to inhabit both fractures and matrix.

completely connect the fracture network and thus activate a more voluminous space for storage [40]. The dissolution and adsorption of CO_2 in local groundwater, organics and clay also consume a certain amount of CO_2, as shown in Fig. 5 (a). Moreover, the historic production of the reservoir generates a pressure drawdown distribution around the well and fractures [162,163]. Injected CO_2 may be preferential to replenish the deficit of pressure in the matrix due to the larger pressure difference. Therefore, increasing the injection scale and wellhead pressure may be necessary to improve the efficiency of CO_2 storage in a single well [86]. The elevation of wellbore pressures, however, should be performed gradually and with care for leakage, since CO_2 fracturing can generate long fractures as reported previously (Case 7, Fig. 2 b).

4.3. Feasibility of symbiotic storage of CO_2 and H_2 in shale

Using CO_2 as a cushion gas for H_2 storage may improve both the permanent sequestration of CO_2 and the periodic injection-recovery of H_2, as presented in Fig. 10. The existence of H_2 in shale reservoirs provides a persistent pressure to drive more CO_2 deeper into the shale matrix, which promotes permanent storage of CO_2. The prior injected CO_2 may swell the shale matrix by the adsorption effects and then compact fractures to enhance the sealing performance for H_2 storage [40,85,86]. The stored CO_2 and native and remaining CH_4 in the reservoir are optimized cushion gases (these could be ~150 % of the stored H_2) to replenish the deficit of reservoir pressure, which is essential to enhance recovery of H_2 [73,164]. A depleted dry shale gas reservoir could be an option for this integrated CO_2 and H_2 storage scheme, which would take advantage of the seal performance in shale reservoirs and avoid the intrinsic problems in using conventional oil reservoirs (dissolution of H_2 and water breakthrough, among others) [165]. This new strategy requires a comprehensive triple-component simulation involving CH_4 production, CO_2 sequestration, and H_2 injection and production [53,73,75,166], as well as research on the chemical and microbial reactions of H_2 in shale. Moreover, CO_2 is expected to be permanently sequestrated in shale reservoirs, whilst H_2 will be cyclicly injected then recovered, repetitively. Further mechanistic studies (for instance, defining CO_2–H_2 multiphase flow in shale fractures) are essential to optimize the scheduling and cycling of the injection-recovery cycle for H_2, in order to improve the recovery rate and purity of H_2 and control the recovery of CO_2.

In this new strategy, CO_2 fracturing is recommended as the technique to allow injection. First, using CO_2 as a fracturing fluid can generate more fractures and then increase the storage capacity due to its high fracturing efficiency (lower volume of injected fluid to generate a microseismic event), as observed in Case 7. Moreover, the higher capacities of pumps (hydraulic power) and wellheads (stress tolerance) for

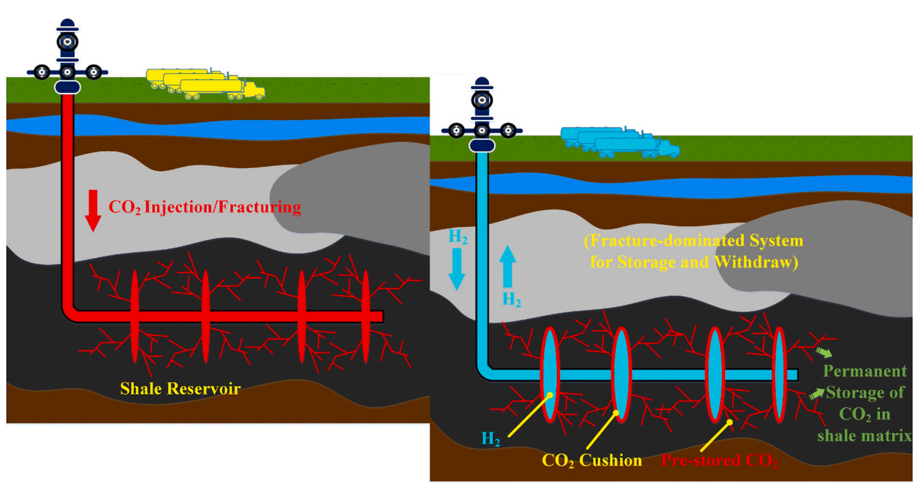

Fig. 10. Conception of symbiotic storage of CO_2 and H_2 in shale reservoirs. CO_2 is used as a cushion gas to replenish the deficit of reservoir pressure for the recovery rate of H_2, which in return drives more CO_2 deeper into the shale matrix for permanent sequestration. Redrawn with permission from Ref. [86], copyright (2021) Elsevier. (This figure has been completely redesigned and redrawn by the authors of the present manuscript).

fracturing, compared with the equipment for flooding or huff and puff stimulation/production, enable the high-pressure injection of CO_2, which increases the percentage retained (Figs. 3 and 6), decreases the recovery of CO_2, and eventually improves the purity and recovery of H_2. However, the proportion of CO_2 utilized in the total fracturing fluid should be increased, and ideally, should reach 100 %. The pumping rate of CO_2 injection should also be increased to enhance proppant transport, fracture propagation, and fracture width [167,168]. An environmentally-friendly and high-efficiency friction reducer is also required to sustain the high-flow-rates necessary for large scale CO_2 injection [86]. The flowback rate of injected CO_2 after fracturing must also be understood and controlled [169,170]. Surface engineering is another bottleneck for fracturing using pure CO_2, including the storage of CO_2 in the field, the capacity of the sealed proppant blender, the provision of real-time supplementary CO_2 for large-scale injection and other factors [171,172]. Therefore, initial breakthroughs in CO_2 fracturing may occur in high payback but water-sensitive reservoirs.

4.4. New evaluation of the prospects of CO_2/H_2 storage in shale

Based on the prior fracture-dominant mechanism, a new evaluation method of CO_2/H_2 storage capacities is proposed based on the scale of fracturing (total volume of injected fluids) in shale reservoirs. The new method assumes that the injection volume of fluids is approximately equal to the volume of created and dilated fractures and then is equivalent to the CO_2/H_2 storage capacity – defined as the equivalent-fracturing method. This method is supported by the apparent effective impermeability of the shale matrix to fracturing fluids, as well as necessary simplifications, such as (1) ignoring the retained fracturing fluids in reservoirs and (2) ignoring the volume of adsorbed CO_2 and H_2. The storage estimate based on this new method is considered to be a minimum although the most technically achievable capacity in shale, referring to the CO_2 injection scales of Cases 1–3 in Table 1. It is also crucial in assessing the capacity of H_2 storage in shales because of the cyclic and repetitive injection and withdrawal process that, due to rapid cycling times, mainly occurs within the fracture network before wholescale diffusion into the matrix can occur.

Taking CO_2 storage as an example, this new method is applied to re-evaluate the storage capacity in Marcellus shale. The total volume of fracturing fluids in Marcellus is estimated by the water usage per fracturing well (an average value of 22,500 m^3) [173–175] and the number of wells drilled annually reported by the Marcellus Center for Outreach and Research (PennState-MCOR) [176]. Thus the newly estimated CO_2 storage capacity in Marcellus shale is 466 million tons as of the year 2019, which is lower than previous estimates (Gt-level) but is still challenging to accomplish because the presumed average CO_2 storage in a single well (22,500 m^3) is much larger than those in field tests (~3265 m^3, Table 1). This new equivalent fracturing method assesses the technically feasible capacity of CO_2 storage in shale, which can be used as a supplement to the evaluation system, and to mitigate the contradiction between the over-estimated CO_2 storage in formation and under-estimation in a single well.

5. Conclusion

A critical review of CO_2 and H_2 storage in shale reservoirs is performed across time and spatial scales. Field cases are critically evaluated with a literature review focusing on field observations and lessons learned, which generate 24 individual lessons from both field pilots and laboratory studies (as presented in Fig. 8). Cross-analyses and validations among these various lessons are performed (as shown in Fig. 8) to demonstrate the principal features of injectivity and sealing behavior in shale reservoirs and the dominance of fracture networks in storing CO_2 and H_2. Perspectives on CO_2 and H_2 storage in shale are proposed by further analyses to pave a broader pathway to carbon neutrality and clean energy transition, which includes.

(1) The fracture-dominated mechanism of CO_2/H_2 storage in shale is clarified. The more isolated nano-scale pores in shale result in a relatively impermeable matrix, in which fracture networks dominate the injection and then the storage capacity. This fracture-dominated system is cross-validated by field measurements (injecting pressures, scales of CO_2, and offset-well monitorings) in previously-fractured and initially-intact shales (Table 1) with the storage behavior of H_2 (mainly stored within fractures) defined as based on numerical simulations (Fig. 7);
(2) An overestimation of CO_2 storage capacity in shale is anticipated. Volumetric and production-based methods of estimation, designed for conventional formations with highly-permeable porous media, may be inapplicable for unconventional reservoirs due to the more isolated nano-scale pores and fracture-dominant mechanisms, as compared in Fig. 9. Hydraulic injection under limited pressure and continuity can only drive CO_2 into the skin of the shale matrix blocks (Case 4 and Fig. 9 b). Furthermore, the injected CO_2 may not follow the direct reverse path of the CH_4 production (deeply into the shale matrix driven by continuous geological stress and pore pressure), which violates a basic assumption for the production-based method and thus results in the overestimation of potential storage volumes;
(3) An underestimation of the scale of the injected CO_2 in the reported field cases is observed and is attributed to the low injecting pressure (indicating that CO_2 mainly concentrates in previously-fractured shales, Case 3) and the low proportion of injected CO_2 (in total injected fluids, Cases 6 and 7), as presented in Table 1. This may result from the unknown characteristics of the fracture networks, the greater penetration of CO_2 as a supercritical fluid and the deficits of pressure and fluids during production – principal factors affecting storage capacity. Among these factors, quantitatively evaluating artificial fractures at field scales is crucial in enhancing the scale of injection of CO_2 in a single well, which represents a promising research orientation;
(4) A new strategy of integrating CO_2 storage and H_2 storage in shale is proposed and then demonstrated by using the same flow path (through fracture networks) of CO_2 and H_2 based on cross-analyses of field tests of CO_2 injection (Table 1 and Fig. 1) and numerical simulations of H_2 storage (Fig. 7). The previously stored CO_2 and remnant CH_4 in a dry gas reservoir can be used as cushion gases to maintain reservoir pressure and thus enhance H_2 recovery (Fig. 10). In this strategy, CO_2 fracturing (with an efficiency ~5 times higher than water-based fracturing, Fig. 2) is recommended for CO_2 storage to increase the fracture volume and the percentage of retention of CO_2 (Figs. 3 and 6) by the increased injecting pressure. This improves the storage capacity in fractures and permanent storage of CO_2 while also maximizing the purity of the recovered H_2. Correspondingly, further studies integrating CH_4 production, CO_2 sequestration, and H_2 injection and then production are essential to reveal the multiphase flow mechanisms in both matrix and fractures, as well as developments in the technical progress for CO_2 fracturing (friction reducer, flow-back control, and surface equipment);
(5) A new equivalent-fracturing method, based on a fracture-dominant mechanism, is proposed and used as a supplement to the evaluation system to mitigate the over- and under-estimations and evaluate the prospect of CO_2 and H_2 storage in shales. Taking CO_2 storage as an example, the new method may be applied to the Marcellus shale and suggests 466 million tons of CO_2 storage capacity in artificial fractures, which is lower than previous estimates (Gt-level that considered storage in both fracture and porous matrix). This fracture-based method estimates a more technically achievable prospect considering the impermeability of the shale matrix, which may improve the injection scale of CO_2 in field pilots.

Declaration of competing interest

The authors declare that they have no known competing financial interests or personal relationships that could have appeared to influence the work reported in this paper.

Data availability

No data was used for the research described in the article.

Acknowledgments

DE acknowledges support from the G. Albert Shoemaker endowment. This research is funded by the National Natural Science Foundation of China under the grants 42377138, 42077247 and 52174107, and the Basic Research and Frontier Exploration Projects in Chongqing (cstc2022ycjh-bgzxm0107). The authors would like to thank Honglei Liu and Xiaobing Bian from SINOPEC, and Weibin Liu from China Geological Survey for their pre-review and comments. Copyright permissions have been attained for all the copyrighted figures and tables.

References

[1] Bui M, Adjiman CS, Bardow A, Anthony EJ, Boston A, Brown S, et al. Carbon capture and storage (CCS): the way forward. Energy Environ Sci 2018;11(5):1062–176.
[2] Furukawa H, Yaghi OM. Storage of hydrogen, methane, and carbon dioxide in highly porous covalent organic frameworks for clean energy applications. J Am Chem Soc 2009;131(25):8875–83.
[3] Leung DYC, Caramanna G, Maroto-Valer MM. An overview of current status of carbon dioxide capture and storage technologies. Renew Sustain Energy Rev 2014;39:426–43.
[4] van Vuuren DP, Stehfest E, Gernaat DEHJ, van den Berg M, Bijl DL, de Boer HS, et al. Alternative pathways to the 1.5 °C target reduce the need for negative emission technologies. Nat Clim Change 2018;8(5):391–7.
[5] Global Change Data Lab. World annual CO_2 emissions from fossil fuels and industry. 2022. Available from: https://ourworldindata.org/co2-dataset-sources.
[6] Global CCS. Carbon capture and storage) Institute. Global Status of carbon capture and storage. 2021. Available from: https://www.globalccsinstitute.com/resources/publications-reports-research/global-status-of-ccs-2021/.
[7] Dong X, Liu H, Chen Z, Wu K, Lu N, Zhang Q. Enhanced oil recovery techniques for heavy oil and oilsands reservoirs after steam injection. Appl Energy 2019;239:1190–211.
[8] Song C, Yang D. Experimental and numerical evaluation of CO2 huff-n-puff processes in Bakken formation. Fuel 2017;190:145–62.
[9] Alvarado V, Manrique E. Enhanced oil recovery: an update review. Energies 2010;3(9):1529–75.
[10] Oil production worldwide from 1998 to 2021 [Internet]. Available from: https://www.statista.com/.
[11] Ozarslan A. Large-scale hydrogen energy storage in salt caverns. Int J Hydrogen Energy 2012;37(19):14265–77.
[12] Andersson J, Grönkvist S. Large-scale storage of hydrogen. Int J Hydrogen Energy 2019;44(23):11901–19.
[13] Furukawa H, Yaghi OM. Storage of hydrogen, methane, and carbon dioxide in highly porous covalent organic frameworks for clean energy applications. J Am Chem Soc 2009;131(25):8875–83.
[14] Schiebahn S, Grube T, Robinius M, Tietze V, Kumar B, Stolten D. Power to gas: technological overview, systems analysis and economic assessment for a case study in Germany. Int J Hydrogen Energy 2015;40(12):4285–94.
[15] Parra D, Valverde L, Pino FJ, Patel MK. A review on the role, cost and value of hydrogen energy systems for deep decarbonisation. Renew Sustain Energy Rev 2019;101:279–94.
[16] Bellosta von Colbe J, Ares J-R, Barale J, Baricco M, Buckley C, Capurso G, et al. Application of hydrides in hydrogen storage and compression: achievements, outlook and perspectives. Int J Hydrogen Energy 2019;44(15):7780–808.
[17] Veluswamy HP, Kumar R, Linga P. Hydrogen storage in clathrate hydrates: current state of the art and future directions. Appl Energy 2014;122:112–32.
[18] Abe JO, Popoola API, Ajenifuja E, Popoola OM. Hydrogen energy, economy and storage: review and recommendation. Int J Hydrogen Energy 2019;44(29):15072–86.
[19] Koohi-Fayegh S, Rosen MA. A review of energy storage types, applications and recent developments. J Energy Storage 2020;27.
[20] Blanco H, Faaij A. A review at the role of storage in energy systems with a focus on Power to Gas and long-term storage. Renew Sustain Energy Rev 2018;81:1049–86.
[21] Moradi R, Groth KM. Hydrogen storage and delivery: review of the state of the art technologies and risk and reliability analysis. Int J Hydrogen Energy 2019;44(23):12254–69.
[22] Jensen SH, Graves C, Mogensen M, Wendel C, Braun R, Hughes G, et al. Large-scale electricity storage utilizing reversible solid oxide cells combined with underground storage of CO2 and CH4. Energy Environ Sci 2015;8(8):2471–9.
[23] Tarkowski R. Underground hydrogen storage: characteristics and prospects. Renew Sustain Energy Rev 2019;105:86–94.
[24] U.S. Energy Information Administration. World Shale Resource Assessments [Internet]. 2015. Available from, https://www.eia.gov/analysis/studies/worldshalegas/.
[25] U.S. Energy Information Administration. 119 publicly traded global oil and natural gas companies added proved reserves in 2021 2022 [Internet], https://www.eia.gov/todayinenergy/detail.php?id=52738.
[26] Zhao C, Ju S, Xue Y, Ren T, Ji Y, Chen X. China's energy transitions for carbon neutrality: challenges and opportunities. Carbon Neutrality 2022;1(1).
[27] Fatah A, Bennour Z, Ben Mahmud H, Gholami R, Hossain MM. A review on the influence of CO2/shale interaction on shale properties: implications of CCS in shales. Energies 2020;13(12).
[28] Iddphonce R, Wang J, Zhao L. Review of CO2 injection techniques for enhanced shale gas recovery: prospect and challenges. J Nat Gas Sci Eng 2020;77.
[29] Rani S, Padmanabhan E, Prusty BK. Review of gas adsorption in shales for enhanced methane recovery and CO2 storage. J Petrol Sci Eng 2019;175:634–43.
[30] Heinemann N, Alcalde J, Miocic JM, Hangx SJT, Kallmeyer J, Ostertag-Henning C, et al. Enabling large-scale hydrogen storage in porous media – the scientific challenges. Energy Environ Sci 2021;14(2):853–64.
[31] Godec M, Koperna G, Petrusak R, Oudinot A. Potential for enhanced gas recovery and CO2 storage in the Marcellus Shale in the Eastern United States. Int J Coal Geol 2013;118:95–104.
[32] Liu D, Li Y, Agarwal R. Evaluation of CO2 storage in a shale gas reservoir compared to a deep saline aquifer in the ordos basin of China. Energies 2020;13(13).
[33] Li W, Zhang M, Nan Y, Pang W, Jin Z. Molecular dynamics study on CO2 storage in water-filled Kerogen nanopores in shale reservoirs: effects of Kerogen maturity and pore size. Langmuir 2021;37(1):542–52.
[34] Busch A, Alles S, Gensterblum Y, Prinz D, Dewhurst DN, Raven M, et al. Carbon dioxide storage potential of shales. Int J Greenh Gas Control 2008;2(3):297–308.
[35] Sampath KHSM, Perera MSA, Ranjith PG, Matthai SK, Rathnaweera T, Zhang G, et al. CH 4 CO 2 gas exchange and supercritical CO 2 based hydraulic fracturing as CBM production-accelerating techniques: a review. J CO2 Util 2017;22:212–30.
[36] Middleton RS, Carey JW, Currier RP, Hyman JD, Kang Q, Karra S, et al. Shale gas and non-aqueous fracturing fluids: opportunities and challenges for supercritical CO2. Appl Energy 2015;147:500–9.
[37] Lu Y, Chen X, Tang J, Li H, Zhou L, Han S, et al. Relationship between pore structure and mechanical properties of shale on supercritical carbon dioxide saturation. Energy 2019;172:270–85.
[38] Jia B, Tsau J-S, Barati R. A review of the current progress of CO2 injection EOR and carbon storage in shale oil reservoirs. Fuel 2019;236:404–27.
[39] Hou L, Elsworth D, Geng X. Swelling and embedment induced by sub- and super-critical-CO2 on the permeability of propped fractures in shale. Int J Coal Geol 2020;225:103496.
[40] Hou L, Elsworth D. Mechanisms of tripartite permeability evolution for supercritical CO2 in propped shale fractures. Fuel 2021:292.
[41] Liu Y, Wilcox J. CO2 adsorption on carbon models of organic constituents of gas shale and coal. Environ Sci Technol 2011;45(2):809–14.
[42] Gilfillan SM, Lollar BS, Holland G, Blagburn D, Stevens S, Schoell M, et al. Solubility trapping in formation water as dominant CO 2 sink in natural gas fields. Nature 2009;458(7238):614–8.
[43] Jin L, Hawthorne S, Sorensen J, Pekot L, Kurz B, Smith S, et al. Advancing CO2 enhanced oil recovery and storage in unconventional oil play—experimental studies on Bakken shales. Appl Energy 2017;208:171–83.
[44] Lei C, Wenzhi T. Application of carbon dioxide miscibel fracturing technology in block G. Chem Eng Oil Gas 2020;49(2):69–72.
[45] Blunt M, Fayers FJ, Orr Jr FM. Carbon dioxide in enhanced oil recovery. Energy Convers Manag 1993;34(9–11):1197–204.
[46] Cao M, Gu Y. Oil recovery mechanisms and asphaltene precipitation phenomenon in immiscible and miscible CO2 flooding processes. Fuel 2013;109:157–66.
[47] Kuang N-j, Zhou J-p, Xian X-f, Zhang C-p, Yang K, Dong Z-q. Geomechanical risk and mechanism analysis of CO2 sequestration in unconventional coal seams and shale gas reservoirs. Rock Mechanics Bulletin 2023;2(4).
[48] Zoback MD. Reservoir Geomechanics. Cambridge: Cambridge University Press; 2007.
[49] Seewald JS. Organic-inorganic interactions in petroleum-producing sedimentary basins. Nature 2003;426(6964):327–33.
[50] Nelson PH. Pore-throat sizes in sandstones, tight sandstones, and shales. AAPG (Am Assoc Pet Geol) Bull 2009;93(3):329–40.
[51] Pfeiffer WT, Bauer S. Subsurface porous media hydrogen storage – scenario development and simulation. Energy Proc 2015;76:565–72.
[52] Zivar D, Kumar S, Foroozesh J. Underground hydrogen storage: a comprehensive review. Int J Hydrogen Energy 2021;46(45):23436–62.
[53] Kanaani M, Sedaee B, Asadian-Pakfar M. Role of cushion gas on underground hydrogen storage in depleted oil reservoirs. J Energy Storage 2022;45.
[54] Bustin RM, Bustin AMM, Cui X, Ross DJK, Pathi VSM, editors. Impact of shale properties on pore structure and storage characteristics, vol. 2008. Society of Petroleum Engineers - Shale Gas Production Conference; 2008.
[55] Jarvie DM, Hill RJ, Ruble TE, Pollastro RM. Unconventional shale-gas systems: the Mississippian Barnett Shale of north-central Texas as one model for

thermogenic shale-gas assessment. AAPG (Am Assoc Pet Geol) Bull 2007;91(4): 475–99.
[56] Loucks RG, Reed RM, Ruppel SC, Jarvie DM. Morphology, genesis, and distribution of nanometer-scale pores in siliceous mudstones of the mississippian barnett shale. J Sediment Res 2009;79(12):848–61.
[57] Gale JFW, Laubach SE, Olson JE, Eichhubl P, Fall A. Natural fractures in shale: a review and new observations. AAPG (Am Assoc Pet Geol) Bull 2014;98(11): 2165–216.
[58] Mayerhofer MJ, Lolon EP, Rightmire C, Walser D, Cipolla CL, Warplnskl NR. What is stimulated reservoir volume? SPE Prod Oper 2010;25(1):89–98.
[59] Gale JFW, Reed RM, Holder J. Natural fractures in the Barnett Shale and their importance for hydraulic fracture treatments. AAPG (Am Assoc Pet Geol) Bull 2007;91(4):603–22.
[60] Ranjith PG, Zhang CP, Zhang ZY. Experimental study of fracturing behaviour in ultralow permeability formations: a comparison between CO2 and water fracturing, vol. 217. Engineering Fracture Mechanics; 2019.
[61] Zhou D, Zhang G, Wang Y, Xing Y. Experimental investigation on fracture propagation modes in supercritical carbon dioxide fracturing using acoustic emission monitoring. Int J Rock Mech Min Sci 2018;110:111–9.
[62] Yushi Z, Xinfang M, Tong Z, Ning L, Ming C, Sihai L, et al. Hydraulic fracture growth in a layered formation based on fracturing experiments and discrete element modeling. Rock Mech Rock Eng 2017;50(9):2381–95.
[63] Chen Y, Nagaya Y, Ishida T. Observations of fractures induced by hydraulic fracturing in anisotropic granite. Rock Mech Rock Eng 2015;48(4):1455–61.
[64] Louk K, Ripepi N, Luxbacher K, Gilliland E, Tang X, Keles C, et al. Monitoring CO2 storage and enhanced gas recovery in unconventional shale reservoirs: results from the Morgan County, Tennessee injection test. J Nat Gas Sci Eng 2017;45: 11–25.
[65] Sorensen JA, Pekot LJ, Torres JA, Jin L, Hawthorne SB, Smith SA, et al. Field test of CO2 injection in a vertical Middle Bakken well to evaluate the potential for enhanced oil recovery and CO2 storage. Proceedings of the 6th Unconventional Resources Technology Conference; 2018.
[66] Jing B, Shan C, Yaohua L, Chang L, Xingyou X, Weibin L. The stimulation mechanism and performance analysis of supercritical CO2 and hydraulic sand-carrying composite volume fracturing technology on continental shale reservoirs. Acta Pet Sin 2022;43(3):399–409.
[67] Yiyu L, Junping Z, Xuefu X, Jiren T, Lei Z, Yongdong J, et al. Research progress and prospect of the integrated supercritical CO2 enhanced shale gas recovery and geological sequestration. Nat Gas Ind 2021;41(6).
[68] Honglei L, Shengqiang X, Biwei Z, Linbo Z, Yajie H, Baolin L. Research and practice of SRV fracturing technology for inter-salt shale oil. Special Oil Gas Reservoirs 2022;29(2).
[69] Singh H. Hydrogen storage in inactive horizontal shale gas wells: techno-economic analysis for Haynesville shale. Appl Energy 2022:313.
[70] Hou L, Cheng Y, Wang X, Ren J, Geng X. Effect of slickwater-alternate-slurry injection on proppant transport at field scales: a hybrid approach combining experiments and deep learning. Energy 2022:242.
[71] Hou L, Wang X, Bian X, Liu H, Gong P. Evaluating essential features of proppant transport at engineering scales combining field measurements with machine learning algorithms. J Nat Gas Sci Eng 2022;107.
[72] Hou L, Ren J, Fang Y, Cheng Y. Data-driven optimization of brittleness index for hydraulic fracturing. Int J Rock Mech Min Sci 2022;159.
[73] Wang G, Pickup G, Sorbie K, Mackay E. Numerical modelling of H2 storage with cushion gas of CO2 in subsurface porous media: filter effects of CO2 solubility. Int J Hydrogen Energy 2022;47(67):28956–68.
[74] Lysyy M, Fernø M, Ersland G. Seasonal hydrogen storage in a depleted oil and gas field. Int J Hydrogen Energy 2021;46(49):25160–74.
[75] Wang G, Pickup G, Sorbie K, Mackay E. Scaling analysis of hydrogen flow with carbon dioxide cushion gas in subsurface heterogeneous porous media. Int J Hydrogen Energy 2022;47(3):1752–64.
[76] Oil base foam fracturing applied to the niobrara shale formationDriscoll PL, Bowen JG, Roberts MA, editors. Proceedings - SPE Annual Technical Conference and Exhibition 1980.
[77] Lillies AT, King SR, editors. Sand fracturing with liquid carbon dioxide. Society of Petroleum Engineers - SPE production technology Symposium; 1982. p. 1982.
[78] Black HN, Langsford RW. Energized fracturing with 50% CO2 for improved hydrobarbon reservoir. J Petrol Technol 1982;34(1):135–40.
[79] Sorensen JA, Hamling JA. Historical Bakken test data provide critical Insights on EOR in tight oil plays: the American oil & gas reporter. 2016. Available from: https://www.aogr.com/.
[80] Hou L, Bian X, Geng X, Sun B, Liu H, Jia W. Incipient motion behavior of the settled particles in supercritical CO2. J Nat Gas Sci Eng 2019;68.
[81] Lan Y, Yang Z, Wang P, Yan Y, Zhang L, Ran J. A review of microscopic seepage mechanism for shale gas extracted by supercritical CO2 flooding. Fuel 2019;238: 412–24.
[82] Sanguinito S, Goodman A, Tkach M, Kutchko B, Culp J, Natesakhawat S, et al. Quantifying dry supercritical CO2-induced changes of the Utica Shale. Fuel 2018; 226:54–64.
[83] Wang L, Yao B, Xie H, Kneafsey TJ, Winterfeld PH, Yin X, et al. Experimental investigation of injection-induced fracturing during supercritical CO2 sequestration. Int J Greenh Gas Control 2017;63:107–17.
[84] Hou L, Sun B, Geng X, Jiang T, Wang Z. Study of the slippage of particle/supercritical CO2 two-phase flow. J Supercrit Fluids 2017;120:173–80.
[85] Hou L, Elsworth D, Geng X. Swelling and embedment induced by sub- and super-critical-CO2 on the permeability of propped fractures in shale. Int J Coal Geol 2020;225:103496.
[86] Hou L, Zhang S, Elsworth D, Liu H, Sun B, Geng X. Review of fundamental studies of CO2 fracturing: fracture propagation, propping and permeating. J Petrol Sci Eng 2021:205.
[87] Edwards RWJ, Celia MA, Bandilla KW, Doster F, Kanno CM. A model to estimate carbon dioxide injectivity and storage capacity for geological sequestration in shale gas wells. Environ Sci Technol 2015;49(15):9222–9.
[88] Ambrose WA, Lakshminarasimhan S, Holtz MH, Núñez-López V, Hovorka SD, Duncan I. Geologic factors controlling CO2 storage capacity and permanence: case studies based on experience with heterogeneity in oil and gas reservoirs applied to CO2 storage. Environ Geol 2008;54(8):1619–33.
[89] Warner NR, Jackson RB, Darrah TH, Osborn SG, Down A, Zhao K, et al. Geochemical evidence for possible natural migration of Marcellus Formation brine to shallow aquifers in Pennsylvania. Proc Natl Acad Sci USA 2012;109(30): 11961–6.
[90] Pruess K. Numerical simulation of CO2 leakage from a geologic disposal reservoir, including transitions from super- to subcritical conditions, and boiling of liquid CO2. SPE J 2013;9(2):237–48.
[91] House KZ, Schrag DP, Harvey CF, Lackner KS. Permanent carbon dioxide storage in deep-sea sediments. Proc Natl Acad Sci USA 2006;103(33):12291–5.
[92] Hosseini M, Ali M, Fahimpour J, Keshavarz A, Iglauer S. Assessment of rock-hydrogen and rock-water interfacial tension in shale, evaporite and basaltic rocks. J Nat Gas Sci Eng 2022;106.
[93] Hosseini M, Fahimpour J, Ali M, Keshavarz A, Iglauer S. Capillary sealing efficiency analysis of caprocks: implication for hydrogen geological storage. Energy Fuel 2022;36(7):4065–75.
[94] Wang J, Wang Z, Sun B, Gao Y, Wang X, Fu W. Optimization design of hydraulic parameters for supercritical CO2 fracturing in unconventional gas reservoir. Fuel 2019;235:795–809.
[95] Zhang X, Lu Y, Tang J, Zhou Z, Liao Y. Experimental study on fracture initiation and propagation in shale using supercritical carbon dioxide fracturing. Fuel 2017; 190:370–8.
[96] Li X, Elsworth D. Geomechanics of CO2 enhanced shale gas recovery. J Nat Gas Sci Eng 2015;26:1607–19.
[97] Xiangzeng W, Jinqiao W, Juntao Z. Application of CO2 fracturing technology for terrestrial shale gas reservoirs. Nat Gas Ind 2014;34(1):64–7.
[98] Baumgärtner J, Zoback MD. Interpretation of hydraulic fracturing pressure-time records using interactive analysis methods. Int J Rock Mech Min Sci 1989;26(6): 461–9.
[99] Wu F, Li D, Fan X, Liu J, Li X. Analytical interpretation of hydraulic fracturing initiation pressure and breakdown pressure. J Nat Gas Sci Eng 2020:76.
[100] Li S, Li Z, Dong Q. Diffusion coefficients of supercritical CO 2 in oil-saturated cores under low permeability reservoir conditions. J CO2 Util 2016;14:47–60.
[101] Wang J, Elsworth D, Wu Y, Liu J, Zhu W, Liu Y. The influence of fracturing fluids on fracturing processes: a comparison between water, oil and SC-CO2. Rock Mech Rock Eng 2017;51(1):299–313.
[102] Garcia DJ, Shao H, Hu Y, Ray JR, Jun Y-S. Supercritical CO2–brine induced dissolution, swelling, and secondary mineral formation on phlogopite surfaces at 75–95 °C and 75 atm. Energy Environ Sci 2012;5(2).
[103] Peck WD, Azzolina NA, Ge J, Bosshart NW, Burton-Kelly ME, Gorecki CD, et al. Quantifying CO2 storage efficiency factors in hydrocarbon reservoirs: a detailed look at CO2 enhanced oil recovery. Int J Greenh Gas Control 2018;69:41–51.
[104] Han J, Park H, Sung W. Relationship between oil recovery and CO2 storage efficiency under the influence of gravity segregation in a CO2 EOR system. Environ Earth Sci 2016;75(1):1–8.
[105] Cui G, Zhu L, Zhou Q, Ren S, Wang J. Geochemical reactions and their effect on CO2 storage efficiency during the whole process of CO2 EOR and subsequent storage. Int J Greenh Gas Control 2021:108.
[106] Bachu S. Review of CO2 storage efficiency in deep saline aquifers. Int J Greenh Gas Control 2015;40:188–202.
[107] Gozalpour F, Ren SR, Tohidi B. CO2 EOR and storage in oil reservoirs. Oil Gas Sci Technol 2005;60(3):537–46.
[108] Farajzadeh R, Eftekhari AA, Dafnomilis G, Lake LW, Bruining J. On the sustainability of CO2 storage through CO2 – enhanced oil recovery. Appl Energy 2020:261.
[109] Narinesingh J, Alexander D, editors. CO2 Enhanced gas recovery and geologic sequestration in condensate reservoir: a simulation study of the effects of injection pressure on condensate recovery from reservoir and CO2 storage efficiency. Energy Procedia; 2014.
[110] Ma L, Fauchille AL, Ansari H, Chandler M, Ashby P, Taylor K, et al. Linking multi-scale 3D microstructure to potential enhanced natural gas recovery and subsurface CO2storage for Bowland shale, UK. Energy Environ Sci 2021;14(8): 4481–98.
[111] Carbon dioxide storage capacity of organic-rich shalesKang SM, Fathi E, Ambrose RJ, Akkutlu IY, Sigal RF, editors. SPE J 2011;16(04):842–55.
[112] Pore structure characterization of North American shale gas reservoirs using USANS/SANS, gas adsorption, and mercury intrusionClarkson CR, Solano N, Bustin RM, Bustin AMM, Chalmers GRL, He L, et al., editors. Fuel 2013;103: 606–16.
[113] Dai J, Zou C, Liao S, Dong D, Ni Y, Huang J, et al. Geochemistry of the extremely high thermal maturity Longmaxi shale gas, southern Sichuan Basin. Org Geochem 2014;74:3–12.
[114] Weniger P, Kalkreuth W, Busch A, Krooss BM. High-pressure methane and carbon dioxide sorption on coal and shale samples from the Paraná Basin, Brazil. Int J Coal Geol 2010;84(3–4):190–205.
[115] Liu Y, Wilcox J. CO2 adsorption on carbon models of organic constituents of gas shale and coal. Environ Sci Technol 2011;45(2):809–14.

[116] Azenkeng A, Mibeck BAF, Kurz BA, Gorecki CD, Myshakin EM, Goodman AL, et al. An image-based equation for estimating the prospective CO2 storage resource of organic-rich shale formations. Int J Greenh Gas Control 2020;98.
[117] Xu R, Zeng K, Zhang C, Jiang P. Assessing the feasibility and CO2 storage capacity of CO2 enhanced shale gas recovery using Triple-Porosity reservoir model. Appl Therm Eng 2017;115:1306–14.
[118] Tao Z, Clarens A. Estimating the carbon sequestration capacity of shale formations using methane production rates. Environ Sci Technol 2013;47(19):11318–25.
[119] Levine JS, Fukai I, Soeder DJ, Bromhal G, Dilmore RM, Guthrie GD, et al. U.S. DOE NETL methodology for estimating the prospective CO2 storage resource of shales at the national and regional scale. Int J Greenh Gas Control 2016;51:81–94.
[120] Jia B, Chen Z, Xian C. Investigations of CO2 storage capacity and flow behavior in shale formation. J Petrol Sci Eng 2022:208.
[121] Chu H, Liao X, Chen Z, Liu W, Mu L, Liu H. A new methodology to assess the maximum CO2 geosequestration capacity of shale reservoirs with SRV based on wellbore pressure. J CO2 Util 2019;34:239–55.
[122] Liu F, Ellett K, Xiao Y, Rupp JA. Assessing the feasibility of CO2 storage in the New Albany Shale (Devonian–Mississippian) with potential enhanced gas recovery using reservoir simulation. Int J Greenh Gas Control 2013;17:111–26.
[123] Kim TH, Cho J, Lee KS. Evaluation of CO2 injection in shale gas reservoirs with multi-component transport and geomechanical effects. Appl Energy 2017;190:1195–206.
[124] Bachu S, Bonijoly D, Bradshaw J, Burruss R, Holloway S, Christensen NP, et al. CO2 storage capacity estimation: methodology and gaps. Int J Greenh Gas Control 2007;1(4):430–43.
[125] Liu D, Li Y, Agarwal RK. Numerical simulation of long-term storage of CO 2 in Yanchang shale reservoir of the Ordos basin in China. Chem Geol 2016;440:288–305.
[126] Myshakin EM, Singh H, Sanguinito S, Bromhal G, Goodman AL. Flow regimes and storage efficiency of CO2 injected into depleted shale reservoirs. Fuel 2019;246:169–77.
[127] Bielicki JM, Langenfeld JK, Tao Z, Middleton RS, Menefee AH, Clarens AF. The geospatial and economic viability of CO2 storage in hydrocarbon depleted fractured shale formations. Int J Greenh Gas Control 2018;75:8–23.
[128] Tayari F, Blumsack S, Dilmore R, Mohaghegh SD. Techno-economic assessment of industrial CO2 storage in depleted shale gas reservoirs. Journal of Unconventional Oil and Gas Resources 2015;11:82–94.
[129] McCoy S, Rubin E. An engineering-economic model of pipeline transport of CO2 with application to carbon capture and storage. Int J Greenh Gas Control 2008;2(2):219–29.
[130] Hepburn C, Adlen E, Beddington J, Carter EA, Fuss S, Mac Dowell N, et al. The technological and economic prospects for CO2 utilization and removal. Nature 2019;575(7781):87–97.
[131] Zhang R-h, Wu J-f, Zhao Y-l, He X, Wang R-h. Numerical simulation of the feasibility of supercritical CO2 storage and enhanced shale gas recovery considering complex fracture networks. J Petrol Sci Eng 2021:204.
[132] Pranesh V. Subsurface CO2 storage estimation in Bakken tight oil and Eagle Ford shale gas condensate reservoirs by retention mechanism. Fuel 2018;215:580–91.
[133] Haddad PG, Ranchou-Peyruse M, Guignard M, Mura J, Casteran F, Ronjon-Magand L, et al. Geological storage of hydrogen in deep aquifers - an experimental multidisciplinary study. Energy Environ Sci 2022;15(8):3400–15.
[134] Tarkowski R, Uliasz-Misiak B, Tarkowski P. Storage of hydrogen, natural gas, and carbon dioxide – geological and legal conditions. Int J Hydrogen Energy 2021;46(38):20010–22.
[135] Heinemann N, Booth MG, Haszeldine RS, Wilkinson M, Scafidi J, Edlmann K. Hydrogen storage in porous geological formations – onshore play opportunities in the midland valley (Scotland, UK). Int J Hydrogen Energy 2018;43(45):20861–74.
[136] Liu W, Zhang Z, Chen J, Fan J, Jiang D, Jjk D, et al. Physical simulation of construction and control of two butted-well horizontal cavern energy storage using large molded rock salt specimens. Energy 2019;185:682–94.
[137] He T, Wang T, Shan B, An G, Yang J, Daemen JJK. Fatigue damage of wellbore cement sheath in gas storage salt cavern under alternating internal pressure. Rock Mech Rock Eng 2022;55(2):715–32.
[138] Liu W, Zhang Z, Fan J, Jiang D, Li Z, Chen J. Research on gas leakage and collapse in the cavern roof of underground natural gas storage in thinly bedded salt rocks. J Energy Storage 2020:31.
[139] Lord AS, Kobos PH, Borns DJ. Geologic storage of hydrogen: scaling up to meet city transportation demands. Int J Hydrogen Energy 2014;39(28):15570–82.
[140] Kruck O, Crotogino F. Assessment of the potential, the actors and relevant business cases for large scale and seasonal storage of renewable electricity by hydrogen underground storage in Europe. 2013. https://hyunder.eu/.
[141] Sainz-Garcia A, Abarca E, Rubi V, Grandia F. Assessment of feasible strategies for seasonal underground hydrogen storage in a saline aquifer. Int J Hydrogen Energy 2017;42(26):16657–66.
[142] Rezaei A, Hassanpouryouzband A, Molnar I, Derikvand Z, Haszeldine RS, Edlmann K. Relative permeability of hydrogen and aqueous brines in sandstones and carbonates at reservoir conditions. Geophys Res Lett 2022;49(12).
[143] Dalal Isfehani Z, Sheidaie A, Hosseini M, Fahimpour J, Iglauer S, Keshavarz A. Interfacial tensions of (brine + H2 + CO2) systems at gas geo-storage conditions. J Mol Liq 2023:374.
[144] Hosseini M, et al. Calcite–fluid interfacial tension: H2 and CO2 geological storage in carbonates. Energy Fuel 2023;37(8):5986–94.
[145] Hosseini M, et al. H2−brine interfacial tension as a function of salinity, temperature, and pressure; implications for hydrogen geo-storage. J Petrol Sci Eng 2022;213:110441.
[146] Hosseini M, Sedev R, Ali M, Ali M, Fahimpour J, Keshavarz A, et al. Hydrogen-wettability alteration of Indiana limestone in the presence of organic acids and nanofluid. Int J Hydrogen Energy 2023 (In Press).
[147] Jia Y, Lu Y, Elsworth D, Fang Y, Tang J. Surface characteristics and permeability enhancement of shale fractures due to water and supercritical carbon dioxide fracturing. J Petrol Sci Eng 2018;165:284–97.
[148] Josh M, Esteban L, Delle Piane C, Sarout J, Dewhurst DN, Clennell MB. Laboratory characterisation of shale properties. J Petrol Sci Eng 2012;88–89:107–24.
[149] Cipolla CL, Lolon EP, Erdle JC, Rubin B. Reservoir modeling in shale-gas reservoirs. SPE Reservoir Eval Eng 2010;13(4):638–53.
[150] Wang H, Chen L, Qu Z, Yin Y, Kang Q, Yu B, et al. Modeling of multi-scale transport phenomena in shale gas production — a critical review. Appl Energy 2020:262.
[151] Loucks RG, Reed RM, Ruppel SC, Hammes U. Spectrum of pore types and networks in mudrocks and a descriptive classification for matrix-related mudrock pores. AAPG (Am Assoc Pet Geol) Bull 2012;96(6):1071–98.
[152] Zou C, Dong D, Wang S, Li J, Li X, Wang Y, et al. Geological characteristics and resource potential of shale gas in China. Petrol Explor Dev 2010;37(6):641–53.
[153] Curtis JB. Fractured shale-gas systems. AAPG (Am Assoc Pet Geol) Bull 2002;86(11):1921–38.
[154] Martin DF, Taber JJ. Carbon dioxide flooding. J Petrol Technol 1992;44(4):396–400.
[155] Zhao H, Xu L, Guo Z, Zhang Q, Liu W, Kang X. Flow-path tracking strategy in a data-driven interwell numerical simulation model for waterflooding history matching and performance prediction with infill wells. SPE J 2019;25(02):1007–25.
[156] Hou L, Cheng Y, Elsworth D, Liu H, Ren J. Prediction of the continuous probability of sand screenout based on a deep learning workflow. SPE J 2022:1–11.
[157] Hou L, Elsworth D, Zhang F, Wang Z, Zhang J. Evaluation of proppant injection based on a data-driven approach integrating numerical and ensemble learning models. Energy 2023;264:126122.
[158] Zhang GQ, Chen M. Dynamic fracture propagation in hydraulic re-fracturing. J Petrol Sci Eng 2010;70(3–4):266–72.
[159] Elbel JL, Mack MG, editors. Refracturing: observations and theories. Production Operations Symposium; 1993.
[160] Warpinski NR, Du J, Zimmer U. Measurements of hydraulic-fracture-induced seismicity in gas shales. SPE Prod Oper 2012;27(3):240–52.
[161] Li L, Tan J, Wood DA, Zhao Z, Becker D, Lyu Q, et al. A review of the current status of induced seismicity monitoring for hydraulic fracturing in unconventional tight oil and gas reservoirs. Fuel 2019;242:195–210.
[162] Shi JQ, Durucan S. Drawdown induced changes in permeability of coalbeds: a new interpretation of the reservoir response to primary recovery. Transport Porous Media 2004;56(1):1–16.
[163] Yin Z, Wan QC, Gao Q, Linga P. Effect of pressure drawdown rate on the fluid production behaviour from methane hydrate-bearing sediments. Appl Energy 2020:271.
[164] Heinemann N, Scafidi J, Pickup G, Thaysen EM, Hassanpouryouzband A, Wilkinson M, et al. Hydrogen storage in saline aquifers: the role of cushion gas for injection and production. Int J Hydrogen Energy 2021;46(79):39284–96.
[165] Torres R, de Hemptinne JC, Machin I. Improving the modeling of hydrogen solubility in heavy oil cuts using an Augmented Grayson Streed (AGS) approach. Oil Gas Sci Technol 2013;68(2):217–33.
[166] Yekeen N, Al-Yaseri A, Negash BM, Ali M, Giwelli A, Esteban L, et al. Clay-hydrogen and clay-cushion gas interfacial tensions: implications for hydrogen storage. Int J Hydrogen Energy 2022;47(44):19155–67.
[167] Hou L, Jiang T, Liu H, Geng X, Sun B, Li G, et al. An evaluation method of supercritical CO2 thickening result for particle transporting. J CO2 Util 2017;21:247–52.
[168] Hou L, Sun B, Wang Z, Li Q. Experimental study of particle settling in supercritical carbon dioxide. J Supercrit Fluids 2015;100:121–8.
[169] Gregory KB, Vidic RD, Dzombak DA. Water management challenges associated with the production of shale gas by hydraulic fracturing. Elements 2011;7(3):181–6.
[170] Llewellyn GT, Dorman F, Westland JL, Yoxtheimer D, Grieve P, Sowers T, et al. Evaluating a groundwater supply contamination incident attributed to Marcellus Shale gas development. Proc Natl Acad Sci USA 2015;112(20):6325–30.
[171] Hou L, Sun B, Li Y, Du Q, Yan L. Impact of unconventional oil and gas exploitation on fracturing equipment and materials development. Nat Gas Ind 2013;33(12):105–10.
[172] Tian L, He J, Yang Z, Wei X. Application of CO2 energized fracturing fluid technology in Jilin oilfield. Drill Fluid Complet Fluid 2015;32(6):78–80.
[173] Kondash AJ, Lauer NE, Vengosh A. The intensification of the water footprint of hydraulic fracturing. Sci Adv 2018;4(8):eaar5982.
[174] Hurdle J. Fracking industry water use rises as drills extend, study says. 2018 [Available from: https://stateimpact.npr.org.
[175] U.S. Geological Survey. Science or Soundbite? Shale gas, hydraulic fracturing, and induced Earthquakes. 2012. Available from: https://www.usgs.gov/.
[176] PennState. Animation of Tri-state shale wells. 2019. Available from: https://marcellus.psu.edu/.